MOLECULAR AND CELLULAR BIOLOGY, Nov. 2007, p. 7365–7380 Vol. 27, No. 21
0270-7306/07/$08.00+0 doi:10.1128/MCB.00331-07

An Intronic Locus Control Region Plays an Essential Role in the Establishment of an Autonomous Hepatic Chromatin Domain for the Human Vitamin D-Binding Protein Gene[▽]

Tomoko Hiroki, Stephen A. Liebhaber, and Nancy E. Cooke*

Departments of Medicine and Genetics, University of Pennsylvania, Philadelphia, Pennsylvania 19104

Received 23 February 2007/Returned for modification 1 April 2007/Accepted 27 August 2007

The human vitamin D-binding protein (hDBP) gene exists in a cluster of four liver-expressed genes. A minimal hDBP transgene, containing a defined set of liver-specific DNase I hypersensitive sites (HSs), is robustly expressed in mouse liver in a copy-number-dependent manner. Here we evaluate these HSs for function. Deletion of HSI, located 5′ to the promoter (kb −2.1) had no significant effect on hDBP expression. In contrast, deletion of HSIV and HSV from intron 1 repressed hDBP expression and eliminated copy number dependency without a loss of liver specificity. Chromatin immunoprecipitation analysis revealed peaks of histone H3 and H4 acetylation coincident with HSIV in the intact hDBP locus. This region contains a conserved array of binding sites for the liver-enriched transcription factor C/EBP. In vitro studies revealed selective binding of C/EBPα to HSIV. In vivo occupancy of C/EBPα at HSIV was demonstrated in hepatic chromatin, and depletion of C/EBPα in a hepatic cell line decreased hDBP expression. A nonredundant role for C/EBPα was confirmed in vivo by demonstrating a reduction of hDBP expression in *C/EBP*α-null mice. Parallel studies revealed in vivo occupancy of the liver-enriched factor HNF1α at HSIII (at kb 0.13) within the hDBP promoter. These data demonstrate a critical role for elements within intron 1 in the establishment of an autonomous and productive hDBP chromatin locus and suggest that this function is dependent upon C/EBPα. Cooperative interactions between these intronic complexes and liver-restricted complexes within the target promoter are likely to underlie the consistency and liver specificity of the hDBP activation.

The vitamin D-binding protein gene (*DBP*) is robustly expressed in the livers of all mammalian species and is under strict developmental control. The *DBP* gene is a member of a gene cluster that includes albumin (*ALB*), α-fetoprotein (*AFP*), and α-albumin/afamin (*AFM*) genes (7). During rodent embryonic development, expression of *ALB*, *AFP*, and *DBP* is induced in yolk sac and is maintained in fetal liver (36), while the hepatic expression of *AFM* is initiated in the perinatal period. *AFP* is selectively silenced at the end of the fetal period, whereas *ALB*, *AFM*, and *DBP* maintain high constitutive levels of expression in adult liver (2). The hDBP protein (also known as Gc-globulin) is secreted from hepatocytes as a polymorphic and multifunctional circulating glycoprotein (232 to 464 μg/ml) (8). In humans, serum DBP is critical to the binding and transport of 25-hydroxyvitamin D, the major circulating form of vitamin D, and 1,25-dihydroxyvitamin D, the most active vitamin D metabolite. DBP also binds tightly to monomeric G-actin, blocking formation of intravascular F-actin networks that can occlude the vasculature following cellular damage (20). Deglycosylated DBP (DBP-maf) may play a role in the innate immune response (reviewed in references 7, 8, and 51) and as a potent antiangiogenic factor (26, 28). These unique functions of DBP suggest roles for DBP in the pathophysiology and treatment of a variety of human disorders (16). The robust expression, developmental control, and wide spectrum of functions of *DBP* establish it as an important model for the analysis of hepatic gene regulation.

The basis for the robust expression of DBP in the hepatocyte is presently under study. Analysis of chromatin structure in hepatocytes has revealed a set of five liver-specific hypersensitive sites (HSs) adjacent to or within the hDBP locus. These studies were carried out in livers from mice carrying a 105-kb hDBP transgene that includes 37 kb of 5′-flanking sequence and 26 kb of 3′-flanking sequence. HSI and HSIII are located 2.1 kb and 0.13 kb upstream of the transcription initiation site, respectively. HSIV and HSV are closely juxtaposed within a 1.9-kb region of intron 1; HSIV maps as a broad band at approximately kb +10.3 through +10.9 and HSV as a more discrete band at kb +12.2. HSVII (at kb +43.9) maps to a site 1.5 kb 3′ to the poly(A) addition site (kb +43.7). Human and rodent genomic comparisons carried out to identify critical *cis*-acting control elements revealed highly conserved noncoding sequences that co-map to these liver-specific HSs. Subsequent analyses revealed that a 51-kb hDBP transgene with minimal flanking sequences (2.5 kb of 5′ sequence and 6.5 kb of 3′ sequence) that encompass the full set of the liver-specific HSs maintains the same level of robust, copy-number-dependent, and liver-specific expression observed for the larger hDBP transgene. These studies of chromatin structure and gene expression support a model in which one or more of the liver-specific HSs constitute components of a liver-specific locus control region (LCR) for the hDBP gene (22). In the present study, this model is tested and further defined. The data led us to conclude that the HS determinants in intron 1 play a major role in the establishment of an autonomous and productive hepatic chromatin locus for hDBP transcription.

* Corresponding author. Mailing address: 547a Clinical Research Building, University of Pennsylvania, 415 Curie Boulevard, Philadelphia, PA 19104. Phone: (215) 898-4425. Fax: (215) 573-5157. E-mail: necooke@mail.med.upenn.edu.

▽ Published ahead of print on 4 September 2007.

TABLE 1. Oligonucleotides and probes used in this study

Oligonucleotide or probe	Sequence(s)
Oligonucleotides	
HaeIII/−2273	5′-ATCATAATTGGCCTAAATGAGAGGCCTCATGTGACAATGATTACTCTAGTAAGTCAGA-3′
HaeIII/−1256	5′-ATCTGTGAAGGTCAATGAAACTAATGAGGCCATTGGAACTCAGTGGAAGAGTTTAAAGAC-3′
EcoRI/7745	5′-AGCCTTAAAAAGAGAAGGAGGGGAATTCTGTCATTTGTGACAACATGGATGACCCTG-3′
EcoRI/14109	5′-CCTGGCTGTCTAAGGGAAGGCTAGGAATTCAGCTGGGGACAAGGTGGAAATCAGGCAAAG-3′
Probes	
Pa	5′-GTTCACAAGGGACATCTGCA-3′, 5′-CATGGCCTATTCAGAGGTCT-3′
Pb	5′-CATCTGGGAAAGGAGGACTTCAC-3′, 5′-CTTAGGGCTTCCATCAAACCAATC-3′
PHSI	5′-GAATCACAGTAAGCAATCAAC-3′, 5′-TAACGTTTTCGTCTCTATTTC-3′
PHSIII	5′-GAGAAGGTGTGCGTTACTAACAT-3′, 5′-TTAATCTCAGAAGCAACACAGAA-3′
P3.4	5′-ACCATCAGAGTGAACAGCAACCTAC-3′, 5′-ACCATCAGAGTGAACAGCAACCTAC-3′
PHSIVa	5′-GGTATACGAATAACTGTTCTAGGGA-3′, 5′-TGGCATAATCTTAGTGACTCTGATG-3′
PHSIVb	5′-ATACCTGGCACAAAGTAAGCCTCAA-3′, 5′-GTACCATTCGGTTATAAAGAAGGTG-3′
P14.9	5′-CATCTGGGAAAGGAGGACTTCAC-3′, 5′-CTTAGGGCTTCCATCAAACCAATC-3′
P29.9	5′-CTTGTTCTGGCTGTATCCTC-3′, 5′-TTGGCCACCCACTTGCTACA-3′
P43.2	5′-GAAACTACCTTCTTGCTTCCAGCC-3′, 5′-TTGAGGAGTGACAGGTATGTTAGT-3′
mGAPDHp	5′-CCTGCCACTGCATCATCGAAC-3′, 5′-GAATGCTACAGTGGGTGAATTG-3′
mPAHp	5′-CCATCTGGGTGGTTGCCTAAGG-3′, 5′-GTTGCCCTGACGTAGCAGTGGA-3′
mTCAMi2	5′-TCTGTCTGAGGTGCAGCTAGAGT-3′, 5′-GTGGTCTAGATCTTGCCACAGATT-3′
f1	5′-CAGAATGTTTCACAATATAGAT-3′ (sense), 5′-ATCTATATTGTGAAACATTCTG-3′ (antisense)
f2	5′-GTGAAAGTGATTTCATCAGAGTCACTAA-3′ (sense), 5′-TTAGTGACTCTGATGAAATCACTTTCAC-3′ (antisense)
mDBPex5	5′-TCTGTATGAGTATTCCAGCA-3′
mDBPex7	5′-TCAGCTAGTGGCAGAACGTT-3′
18S rRNA	5′-CGGCATGTATTAGCTCTAGAATTACCACAG-3′

Furthermore, evidence is presented to support complementing roles for the liver-enriched *trans*-acting factors C/EBPα and HNF1α in this process.

MATERIALS AND METHODS

Materials. Restriction and modification enzymes were purchased from New England Biolabs (Beverly, MA), Life Technologies (Rockville, MD), and Roche Molecular Biochemicals (Indianapolis, IN). [α-^{32}P]dCTP, [γ-^{32}P]ATP, MicroSpin G-50 columns, and Ready-To-Go DNA-labeled beads were purchased from Amersham Biosciences (Piscataway, NJ). Random-primed DNA labeling kits and *Taq* DNA polymerase were from Roche Molecular Biochemicals. QIAEX II and RNeasy mini kits were from QIAGEN. Elutip columns were from Schleicher and Schuell (Keene, NH), and RNAzol B RNA isolation solvent was from TEL-TEST, Inc. (Friendswood, TX). Zeta-Probe nylon membranes were from Bio-Rad (Hercules, CA).

Oligonucleotides. The various oligonucleotides used are listed in Table 1. These were synthesized either by Life Technologies, Inc., or by the DNA Sequencing Facility of the University of Pennsylvania.

Preparation of DNA probes. The DNA probes for genomic Southern blots and Northern blots were released as EcoRI fragments from the human (6) *DBP* cDNA plasmids. The MX probe, which detects the unique 3′-flanking region of the mouse ζ-globin gene, was released as a 1.3-kb BamHI fragment from the pMX plasmid (33). The mouse ribosomal protein L32 (mrpL32) cDNA probe was released as a 0.32-kb EcoRI and HindIII fragment from the mrpL32 plasmid (34). The probes used for DNase I mapping were generated by PCR using *Taq* DNA polymerase. The templates for the PCR were PAC clones 231M2 and 45P24 (43). Each fragment was recovered from an agarose gel using a QIAEX II kit and labeled with [α-^{32}P]dCTP using a random-primed DNA labeling kit or Ready-To-Go DNA-labeled beads. Fragments were then purified on MicroSpin G-50 columns.

Deletion of HSI and the HSIV-HSV region from the 51-kb hDBP transgene. The hDBP-45P24 PAC clone contains a 123-kb insert carrying the hDBP gene along with 2.5 kb of 5′-flanking sequence and 78 kb of 3′-flanking sequence (43). The 51-kb hDBP transgene, reported previously (22), can be released from the hDBP-45P24 PAC clone by double digestion with NotI and FspI. The released 51-kb hDBP gene was inserted into the PAC vector to generate the 51-kb hDBP PAC. The DNA segment between two HaeIII sites (bp −2273 and −1256) encompassing HSI and the DNA segment between two EcoRI sites (bp +7745 and +14109 in intron 1) encompassing HSIV and HSV were individually deleted from the 51-kb hDBP to generate the 50-kb hDBP(ΔHSI) and the 45-kb hDBP(ΔHSIV,V) transgenes, respectively (Fig. 1A). Selective cleavage at the two HaeIII or EcoRI sites in this PAC plasmid was carried out by RecA-assisted restriction endonuclease (RARE) cleavage (1, 4, 13, 37). In the presence of the bacterial protein RecA, oligonucleotides were used to hybridize to specific restriction sites in the PAC clone, thereby protecting them from methylation by HaeIII or EcoRI DNA methylase. After inactivation of RecA and the methylase, the protected restriction sites in the PAC clone were digested with HaeIII or EcoRI. Each RARE cleavage reaction mixture contained 5× RecA buffer (32 μl [125 mM Tris acetate, pH 7.85, 20 mM $MgCl_2$, 2.5 mM spermidine hydrochloride, 2 mM dithiothreitol]), ADP (16 μl [11 mM]), ATP-γ-S (16 μl [3 mM]), RecA protein (20 μl [2 mg/ml]; New England Biolabs), 60-mer oligonucleotides (4.5 μl; 160 ng/μl each) (HaeIII/−2273, HaeIII/−1256, EcoRI/7745, or EcoRI/14109) (Table 1), and distilled H_2O (to achieve a final volume of 160 μl). These reagents were mixed and prewarmed to 37°C for 1 min. PAC plasmid (4 μg in Tris-EDTA [TE]) and acetylated bovine serum albumin (1.6 μl [10 mg/ml]; New England Biolabs) were added, and the incubation was continued at 37°C for 20 min. HaeIII or EcoRI methylase (8 μl [4 U/μl]) and *S*-adenosylmethionine (8 μl [4 U/μl]; New England Biolabs) were then added. After incubating at 37°C for 60 min, RecA protein and methylase were denatured by incubating the mixture at 65°C for 15 min. Methylated DNA was dialyzed on filters (0.025 μm [VS]; Millipore, Bedford, MA) against 0.5× TE for 30 min and then cleaved with HaeIII or EcoRI for 2 h at 37°C.

The RARE cleavage products were separated by field-inversion gel electrophoresis (FIGE) on 1% low-melting-point agarose gels (SeaPlaque GTG-agarose; FMC Bioproducts, Rockland, ME). The modified DNA fragment was purified from a gel slice using gelase (Epicenter Technologies, Madison, WI) (37), religated, and then transformed into *Escherichia coli* DH10B (Life Technologies, Inc.). The transformed cells were then plated on agar plates containing kanamycin and incubated at 37°C for 16 h. The desired clones were selected after analysis by Southern blotting or PCR using probes or primers representing the deleted fragments. Finally, the modified PAC clones were sequenced across the deletion sites to confirm that the RARE cleavage occurred at the desired positions.

Generation of transgenic mice. The 50-kb hDBP(ΔHSI) and 45-kb hDBP (ΔHSIV,V) transgene fragments were released from vector sequences by NotI digestions, and fragments were separated by FIGE using 1% low-melting-point agarose gels (SeaPlaque GTG-agarose; FMC BioProducts, Rockland, ME). Each insert was isolated from a gel slice, phenol extracted, ethanol precipitated, and purified by Elutip. The DNA was then diluted to 2 ng/μl in a mixture of 10 mM

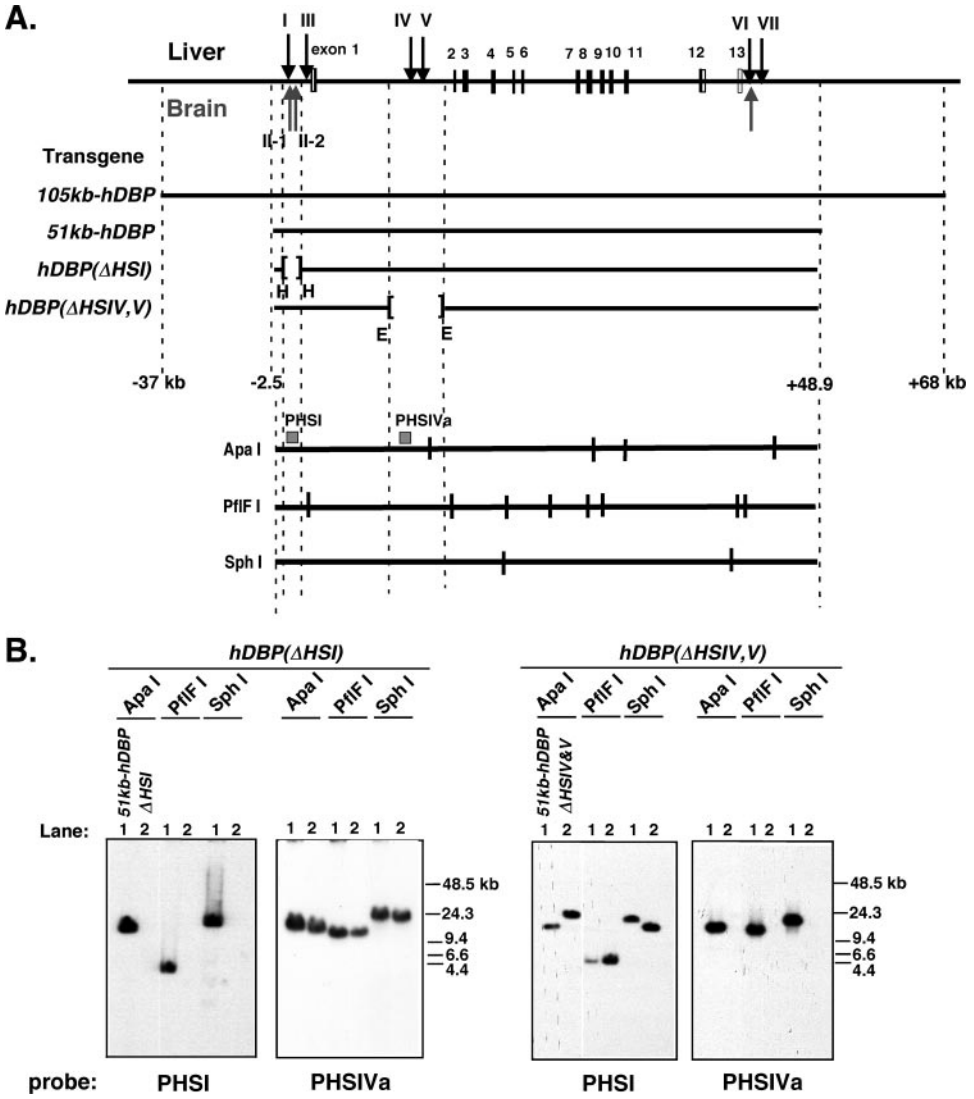

FIG. 1. Physical map of the hDBP gene locus and positions of the targeted deletions of HSI and HSIV and HSV. (A) Diagram of the hDBP gene locus and transgenes. A physical map of the hDBP gene is shown at the top of the figure with the full set of DNase I HSs that were previously identified by analysis of liver and brain chromatin from the 105-kb hDBP transgenic mice (22). Vertical arrows above and below the map indicate the positions of the HSs in the liver and brain, respectively. The transgenes used in the current studies are drawn below the physical map: the two native hDBP transgenes, 105-kb hDBP and 51-kb hDBP, and the deletion mutation transgenes derived from the 51-kb hDBP, 50-kb hDBP(ΔHSI) and 45-kb hDBP(ΔHSVI,V). The hDBP(ΔHSI) and hDBP(ΔHSVI,V) transgenes were created by the deletion of either a 1.0-kb HaeIII (H) fragment encompassing HSI or a 6.4-kb EcoRI (E) fragment encompassing HSIV-HSV from the 51-kb hDBP transgene using the RARE cleavage approach (see Materials and Methods). The restriction enzyme maps of ApaI, PflFI, and SphI and the positions of probes PHSI and PHSIVa (gray rectangles) (sequences in Table 1) used in panel B (below) to confirm the structures of the two sets of deleted transgenes are shown. (B) Confirmation of the structures of the hDBP(ΔHSI) and hDBP(ΔHSVI,V) transgenes. The 51-kb hDBP PAC plasmid (lanes 1) and hDBP(ΔHSI) or hDBP(ΔHSVI,V) PAC inserts (lanes 2) were released from the vector with NotI and then digested with ApaI, PflFI, or SphI and analyzed by Southern blotting with labeled probe PHSI or PHSIVa (shown in panel A). In the left panels, the hybridization patterns of the 51-kb hDBP PAC are as expected (lanes 1) and the analysis of the hDBP(ΔHSI) confirms the deletion of the HSI region. The analysis with the PHSIVa probe confirms that the HSIV-HSV region remained intact. The ApaI and SphI fragments of hDBP(ΔHSI) PAC plasmids were ~1 kb shorter than those of the intact 51-kb hDBP plasmid, whereas the PflFI digestions with probe PHSIVa resulted in bands of identical sizes. The two panels on the right show the corresponding analysis of the hDBP(ΔHSIV,V). Hybridization with the PHSI probe revealed that the hybridizing ApaI fragment is ~9.5 kb longer than that of the intact 51-kb hDBP plasmid, as predicted. Similarly, the SphI fragment of hDBP(ΔHSIV,V) was 6.4 kb shorter than that of the 51-kb hDBP plasmid, and the lengths of PflFI fragments of both constructs were identical. The intact 51-kb hDBP plasmid had the expected bands with probe PHSIVa, whereas there were no signals with this probe in the hDBP(ΔHSIV,V) plasmid. These restriction patterns corresponded precisely to the predictions of the restriction maps in panel A and demonstrated the accuracy of the targeted deletions of the HSI and HSIV-HSV regions.

Tris-HCl (pH 7.6) and 0.1 mM EDTA and microinjected into fertilized mouse oocytes. Transgenic founders were identified by dot blot or PCR analyses of tail DNA samples, and transgene copy number was determined for each line by Southern blot analysis. All animal work was carried out under protocols approved by the University of Pennsylvania Institutional Animal Care and Usage Committee.

Southern blot analyses. Ten to 15 μg of restriction enzyme-digested mouse tail DNA was analyzed on 1.0% agarose gels, transferred to Zeta-Probe membrane with 10× SSC (1× SSC is 1.5 M NaCl plus 0.15 M sodium citrate), and UV cross-linked to the membrane. The membrane was prehybridized for 16 h under standard conditions, washed in 0.5× SSC–0.1% sodium dodecyl sulfate (SDS) at room temperature (RT) and finally 0.1× SSC–0.1% SDS at 65°C, and exposed to XAR-5 films (Kodak). Signals were quantified by PhosphorImager (Molecular Dynamics, Inc., Sunnyvale, CA), and transgene copy number was determined as previously described (22).

Northern blot analyses. Five to 20 μg of total RNA was denatured at 55°C, separated in 1.5% agarose-formaldehyde gels, and transferred to Zeta-Probe membrane with 10× SSC. After UV cross-linking, the blots were prehybridized and subsequently hybridized with ^{32}P-labeled probes at 42°C for 16 h. The membranes were washed with 2× SSC–0.1% SDS at room temperature and finally 0.1× SSC–0.1% SDS at 65°C. The washed membranes were exposed to XAR-5 films (Kodak), and signals were quantified by PhosphorImager. Total liver RNAs from wild-type (WT), *C/EBPα*$^{+/-}$, and *C/EBPα*$^{-/-}$ mice (postnatal day 1) were generous gifts from Klaus Kaestner (University of Pennsylvania); total RNA samples from livers of wild-type and *C/EBPβ*$^{-/-}$ mice (adult) were generous gifts from Linda E. Greenbaum (University of Pennsylvania). mDBPex5 and mDBPex7 (Table 1) were used to generate the mouse *DBP* cDNA probe for *C/EBP*-null mouse analyses by reverse transcription-PCR.

RID assay. For the radial immunodiffusion (RID) assay, 1% agarose containing 3% rabbit polyclonal anti-hDBP (Cocalico Biologicals, Inc., Reamstown, PA) was poured onto a glass backing, and circular wells were cut into the solidified matrix. Test mouse sera and the standard sera containing hDBP protein (Calbiochem, Inc., San Diego, CA) (2 to 4 μl) were loaded into each well and allowed to diffuse for 40 h at RT. The gels were rinsed first with phosphate-buffered saline (PBS) for 16 h and then with distilled water for 20 h. Gels were stained with 0.1% Coomassie brilliant blue in 50% methanol and 10% acetic acid for 30 min and subsequently destained with 50% methanol and10% acetic acid for 1 h. The amount of hDBP in each serum sample was obtained by comparing the diameters of the stained immunodiffused circles of each test serum and the hDBP standard sera at dilutions of 50 to 500 μg/ml.

Isolation of intact nuclei. Livers were perfused with cold PBS and minced, and nuclei were isolated as described previously (17). The nuclear pellets were resuspended in buffer D (15 mM Tris-HCl [pH 7.4], 15 mM NaCl, 60 mM KCl, 0.5 mM EGTA, 0.5 mM β-mercaptoethanol, 0.5 mM spermidine, 0.5 mM spermine). Brains of transgenic mice were washed in PBS, and cells were dissociated in cell-free dissociation buffer (GIBCO-BRL, Grand Island, NY). Cells were lysed in NB3 buffer consisting of 320 mM sucrose, 1 mM $MgCl_2$, 0.05% Triton X-100, 1 mM PIPES [*N*,*N*′-bis(2-ethanesulfonic acid) (pH 6.4)], and 0.1 mM phenylmethylsulfonyl fluoride (PMSF). Nuclei were washed in RB buffer (0.1 M NaCl, 50 mM Tris-HCl [pH 8.0], 3 mM $MgCl_2$, 0.1 mM PMSF, 5 mM sodium butyrate), pelleted, and resuspended in RB buffer.

DNase I hypersensitivity mapping. The concentrations of nuclei were estimated from measurements of A_{260}/A_{280}. Five hundred micrograms of liver nuclei was suspended in buffer D with 5 mM $MgCl_2$ and incubated on ice for 10 min with increasing amounts of DNase I (Life Technologies). EDTA was added to a 25 to 50 mM final concentration to terminate the reactions. The DNase I-digested liver nuclei were incubated in lysis buffer (800 mM NaCl, 0.5% SDS, 100 μg/ml proteinase K) at 55°C overnight. The lysed liver nuclei samples were extracted with phenol and chloroform, and the DNAs were precipitated with ethanol and suspended in TE buffer. The DNAs were subsequently digested with appropriate restriction enzymes, resolved by electrophoresis on 0.8 to 1.0% agarose gels, and transferred to Zeta-Probe membranes for Southern blot analysis.

Cell culture and preparation of crude nuclear extract. HepG2 and Hep3B cells (American Type Culture Collection) were cultured in Eagle's minimal medium supplemented with 2 mM L-glutamine, 100 IU/ml penicillin, 100 μg/ml streptomycin (Life Technologies), and 10% fetal bovine serum. Nuclear extracts of HepG2 and HepB3 cells and mouse livers were prepared as described previously (12), except that all of the solutions contained a protease inhibitor cocktail (Sigma).

EMSA. Electrophoretic mobility shift assay (EMSA) probe fragments f1 and f2 (see Fig. 6A) were generated by annealing complementary synthetic oligonucleotides and then 5′-end labeling the duplex with [γ-^{32}P]ATP and T4 polynucleotide kinase. Radiolabeled probe fragments were gel purified on 10% polyacrylamide gels. Binding reaction mixtures (25 μl) contained 10,000 cpm of the labeled double-stranded DNA fragments (0.2 ng) in binding buffer consisting of 10 mM HEPES (pH 7.9), 1 mM EDTA, 1 mM dithiothreitol, 0.1 M KCl, 5% glycerol, 0.08 mg/ml poly(dI-dC), and 0.3 mg/ml bovine serum albumin. Nuclear extract (2 μg) was added last, and the reaction mixture was incubated at RT for 20 min. In some samples, unlabeled DNA fragment (40 ng [200-fold]) was added as competitor prior to the addition of nuclear extract. For supershift assays, 2 μg of polyclonal antibody to C/EBPα or C/EBPβ (sc-61X and sc-150X; Santa Cruz Biotechnology, Inc., Santa Cruz, CA) was added at the end of the initial 20-min binding reaction, and the reaction mixture was incubated for an additional 30 min. The specificity of these antibodies has been previously validated (10, 42). Samples were resolved on a 5% nondenaturing polyacrylamide gel in 1× Tris-borate-EDTA (TBE) buffer. Gels were dried and exposed to X-ray film at RT.

siRNA interference. si*GENOME SMART*pool small interfering RNA (siRNA) for targeting C/EBPα mRNA (a pool of four designed siRNA duplexes; catalog no. M-006422-01) and *siCONTROL* lamin A/C siRNA (catalog no. D-001050-01; Dharmacon, Inc., Lafayette, CO) were used in the knockdown studies (3). Hep3B cells were seeded in antibiotic-free medium 24 h prior to transfection. The siRNAs (100 nM) or "mock RNAs" were transfected into Hep3B cells using Oligofectamine 2000 (Invitrogen) according to the manufacturer's instructions. An additional siRNA transfection was performed 48 h later to extend the mRNA knockdown to 72 h (see Results). The effectiveness of the target mRNA reduction was monitored by Northern and/or Western blot analyses. The human C/EBPα cDNA probe was released as a 0.47-kb EcoRI and NotI fragment from C/EBPα pcDNA3 vector (Linda E. Greenbaum, University of Pennsylvania). For Western blot analyses, whole-cell protein extracts were prepared with the lysis buffer (10 mM Tris-HCl [pH 7.4], 1% NP-40, 0.1% sodium deoxycholate, 0.1% SDS, 0.15 M NaCl, 1 mM EDTA) supplemented with protease inhibitors. Total protein (30 to 50 μg) was loaded on 10% SDS-polyacrylamide gel electrophoresis for each sample, and Western blots were incubated with anti-DBP (A0021; Dako A/S, Carpinteria, CA), anti-lamin A/C (2032; Cell Signaling), and biotin-conjugated antiactin (sc-1616B; Santa Cruz) antibodies. Secondary antibodies were horseradish peroxidase-conjugated antibiotin (7075; Cell Signaling) and horseradish peroxidase-conjugated anti-rabbit immunoglobulin G (IgG) (Amersham Biosciences). The lamin A/C siRNA effect was verified by Western blot analysis (data not shown).

Immunoprecipitation of unfixed chromatin. The chromatin immunoprecipitation (ChIP) assay was carried out as described previously (27) with minor modifications. Liver or brain nuclei (0.5 mg) were digested with 5 U of micrococcal nuclease (Amersham Biosciences, Picataway, NJ) at 37°C for 10 min in 1 ml digestion buffer. The reaction was terminated by addition of EDTA to a final concentration of 0.5 mM, and salt-soluble chromatin was isolated as described previously (21). Soluble chromatin was concentrated using Microcon centrifugal filters (Millipore Corp., Bedford, MA). The concentrated chromatin was diluted twofold by adding immunoprecipitation buffer. It was next precleared with 50 mg protein A-Sepharose beads (Amersham Biosciences) for 2 h at 4°C with gentle rotation. Twenty percent of the resulting soluble chromatin was kept as the input fraction. The input fraction was composed of DNA fragments sized at ~500 to 1,500 bp. The immunoprecipitation reaction was performed on the precleared chromatin by adding 20 μl of ChIP-grade anti-acetyl histone H3 (06-599; Upstate Biotechnology, Inc., Lake Placid, NY) or ChIP-grade anti-acetyl histone H4 (06-866; Upstate Biotechnology) and incubating the sample overnight at 4°C with gentle rotation. The immune complexes were collected by incubation with 50 mg protein A-Sepharose beads (Amersham Biosciences) for 2 h at 4°C with gentle rotation. The beads were washed three times with 10 ml buffer A containing increasing amounts of NaCl to 150 mM. Bound fractions were eluted twice by incubating the beads in 0.3 ml buffer A containing 1% SDS. Bound fractions were treated with 20 μg of proteinase K, and DNA was phenol extracted from the input and the bound fractions. The purified and precipitated DNAs were resuspended in water, and sequential dilutions of input and bound DNAs were analyzed by PCR (Table 1) to confirm that each assay was within the linear range of amplification. PCR products were resolved through 1.0% agarose gels and analyzed by Southern blotting. Signal intensities were quantified with the PhosphorImager. Ratios between bound and input fractions were obtained within a linear PCR amplification range. Each ratio was normalized to the comparable signal detected at the ubiquitously expressed mouse glyceraldehyde-3-phosphate dehydrogenase (mGAPDH) promoter (defined as 1.0).

Immunoprecipitation of fixed chromatin. Perfused livers of the 105-kb hDBP transgenic mice were minced and fixed in 1% formaldehyde–PBS at RT for 10 min followed by the addition of glycine (0.125 M) with incubation at RT for an additional 5 min. The fixed material was then washed with cold PBS containing 1 mM PMSF and protease inhibitors (Roche, Indianapolis, IN) and Dounce homogenized in cold cell lysis buffer (10 mM Tris-HCl [pH 8.0], 10 mM NaCl, 3

mM $MgCl_2$, 0.5% NP-40) supplemented with protease inhibitors. Cells were incubated at 4°C for 10 min to allow the release of nuclei. Pelleted nuclei were suspended in SDS lysis buffer (50 mM Tris-HCl [pH 8.1], 10 mM EDTA, 1% SDS, 10 mM sodium butyrate, 1 mM PMSF) with protease inhibitors incubated on ice for 10 min. The lysates were then sheared (Sonic Dismembrator; Fisher Scientific) to an average size of 1 kb. The ChIP was performed following the instructions of Upstate Biotechnology. Briefly, an aliquot of soluble chromatin was diluted 10-fold in ChIP dilution buffer with protease inhibitors and precleared with 80 μl of protein A-agarose slurry for 1 h at 4°C with gentle rotation, and an aliquot of each sample was used as "input" in the PCR analysis. The remainder of the soluble chromatin was incubated at 4°C overnight with 20 to 30 μg of C/EBPα (sc-61X) (11, 35, 52), C/EBPβ (sc-150X) (11, 25, 35, 52, 53), HNF1α (sc-6547X) (25, 40), and HNF1β (sc-7411X) (25, 49) antibodies (Santa Cruz Biotechnology) or preimmune IgG (Upstate Biotechnology). Immune complexes were collected by incubation with 60 μl of protein A-agarose slurry for 2 h at 4°C with gentle rotation. The complexes were serially washed in 1 ml of low-salt buffer, high-salt buffer, and LiCl buffer and twice with TE. The complexes were eluted twice with two 250-μl aliquots of elution buffer (1% SDS, 0.1 M $NaHCO_3$). DNA was isolated by reversing the cross-links; samples were heated at 65°C for 5 h in the presence of 0.2 M NaCl and subsequently digested with 20 μg of proteinase K. DNA was isolated from the input and the bound fractions by phenol-chloroform extraction and ethanol precipitation. The purified DNA was resuspended in water. PCR (Table 1), Southern blots, and quantification were performed as described above.

Sequence analysis. Sequence alignment was performed using MacVector 7.2, and potential transcription factor DNA binding sites were analyzed using Match public version 1.0.

RESULTS

Generation of the hDBP(ΔHSI) and hDBP(ΔHSIV,V) transgenic mouse lines. The previously reported 51-kb hDBP transgene is sufficient to direct liver-specific, high-level, copy-number-dependent expression of the hDBP gene in transgenic mouse liver (22). All five liver-specific HSs identified at the hDBP genomic locus are encompassed in this minimal 51-kb hDBP transgene (Fig. 1A). Determinants critical to the activated hDBP chromatin locus were identified by introducing site-specific deletions within the 51-kb hDBP transgene. A 1.0-kb segment encompassing HSI and a 6.4-kb segment encompassing HSIV and HSV were separately deleted from the 51-kb hDBP transgene by RARE cleavage (see Materials and Methods). The overall structures of the resultant 50-kb hDBP(ΔHSI) and the 45-kb hDBP(ΔHSIV,V) PAC plasmids were confirmed by restriction enzyme mapping with Southern blotting, targeted PCR, and selective DNA sequencing (Fig. 1A and B) (data not shown). The two genomic inserts were released from the PAC vector and microinjected into single-cell mouse zygotes. Four hDBP(ΔHSI) lines and seven hDBP(ΔHSIV,V) lines were generated. The transgene copy number for each line was determined by Southern analysis (data not shown).

DNase I HS mapping of hDBP(ΔHSI) and hDBP(ΔHSIV,V) transgenic mice. Removal of the targeted HS was confirmed by DNase I mapping (Fig. 2). Control studies confirmed the presence of HSI, HSIII, HSIV, and HSV at the native 51-kb hDBP transgene locus (Fig. 2B and C). High-resolution mapping of the 5′-flanking 3.8-kb XcmI fragment revealed that HSIII (at kb −0.13) was composed of two sub-bands. Deletion of the HSI region in the hDBP(ΔHSI) mice decreased the XcmI fragment by the predicted 1 kb. The analysis of a liver chromatin sample from the hDBP(ΔHSI) mice confirmed loss of HSI, while formation of HSIII, HSIV, and HSV was retained (Fig. 2B and C). Analysis of liver chromatin from the hDBP(ΔHSIV,V) mice revealed the expected decrease in the size of the intron 1 fragment to 7.5 kb along with loss of HSIV and HSV and retention of HSI formation (Fig. 2B and C). Thus, the two sets of deletions mapped correctly in the corresponding sets of transgenic mice and the targeted HSs were successfully and selectively removed.

Impact of deletions of HSI and of HSIV-HSV on hDBP transgene expression. The tissue distributions of hDBP(ΔHSI) and hDBP(ΔHSIV,V) transgene expression were determined by Northern blotting. Liver-specific expression of hDBP mRNA was observed in both deletion lines. hDBP mRNA was also detected in the intestines at trace levels (Fig. 3A). Overall, the tissue distributions of hDBP expression from the hDBP(ΔHSI) and hDBP(ΔHSIV,V) transgenes were consistent with that previously reported for the native 51-kb hDBP transgene (22).

hDBP expression was quantified in livers of adult male mice carrying HS deletions. mRNA levels, determined by Northern blots, were normalized to endogenous mouse ribosomal protein L32 (mrpL32) mRNA and to the corresponding transgene copy numbers (Fig. 3B). Expression in the four hDBP(ΔHSI) lines was comparable to that in the native hDBP (WT) line (955B). In addition, the levels of expression were copy number dependent, varying by less than twofold within the set. In contrast, deletion of HSIV and -V resulted in a decrease in expression as well as a loss of transgene copy number dependence. hDBP mRNA expression from six of the seven hDBP(ΔHSIV,V) lines was substantially lower than levels observed with the 51-kb hDBP transgene. Of note, in the three single-copy lines (1099G, 2018F, and 2018G) hDBP mRNA expression was at trace levels compared to the robust expression in the single-copy hDBP(ΔHSI) line (2004C). Liver hDBP mRNA levels per copy number in the full set of seven hDBP(ΔHSIV,V) lines ranged over 36-fold. Thus, the hDBP(ΔHSIV,V) transgene had the lost copy number dependency characteristic of the native hDBP transgene locus.

There is very little posttranslational regulation of DBP, so protein levels are a good alternative index of gene expression. Therefore, expression of the hDBP(ΔHSI) and hDBP(ΔHSIV,V) transgenic lines was also determined at the level of protein production from a more comprehensive set of animals, including males and females. Serum hDBP was measured by RID assay and by enzyme-linked immunosorbent assay (ELISA) and compared to values obtained from the native 105-kb hDBP and 51-kb hDBP lines (Fig. 4A). The serum hDBP levels per transgene copy in the 105-kb hDBP and 51-kb hDBP lines ranged from 85 to 233 μg/ml/copy and 80 to 189 μg/ml/copy, respectively (22). These levels are within the range of DBP in normal human serum (116 to 232 μg/ml/copy) (8). The serum hDBP levels/transgene copy in the four hDBP(ΔHSI) lines were comparable to the lower level of normal observed for the native hDBP lines and were tightly grouped within a 1.3-fold range. In contrast, the mean hDBP level in the hDBP(ΔHSIV,V) lines was lower and more variable than in the intact or ΔHSI lines and was reduced to 20% of that of the controls ($P < 0.05$). Whereas the expression in one line (1072H [60 μg/ml/copy]) was comparable to the lower levels in the native 51-kb hDBP lines, the levels of the other three multicopy lines (37, 33, and 26 μg/ml/copy) were significantly lower. Expression levels from the three single-copy lines were decreased even more dramatically (4 to13 μg/ml/copy), while

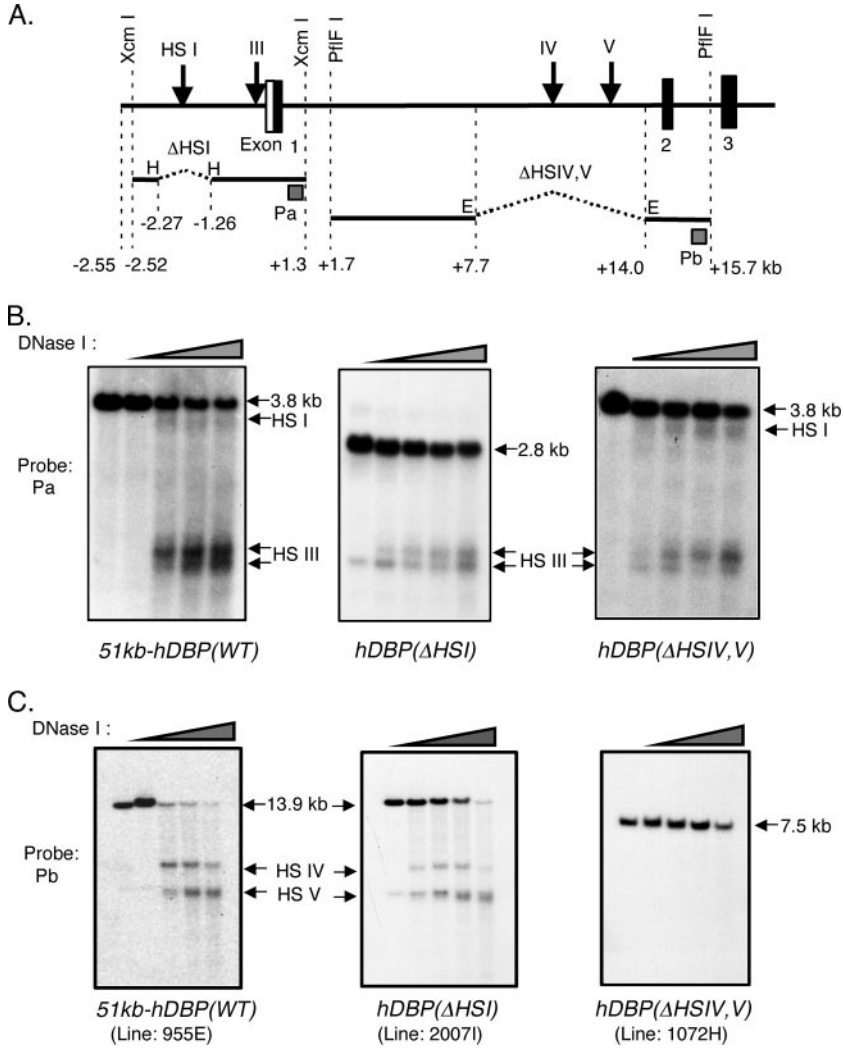

FIG. 2. HSI and HSIV-HSV in hepatic chromatin were eliminated from the hDBP transgenes by the targeted deletions. (A) DNase I mapping strategy and summary of results. Nuclei were isolated from livers of the 51-kb hDBP (WT), hDBP(ΔHSI), and hDBP(ΔHSIV,V) transgenic mice. Liver nuclei were digested with increasing amounts of DNase I followed by complete digestion with XcmI (B) or PflFI (C). These fragments were analyzed by Southern blotting using labeled probe Pa or Pb (gray rectangles). The positions of DNase I HS cleavage deduced from these studies are shown on the map in relation to the positions of the deletions. (B) Selective inactivation of HSI in hepatic chromatin of hDBP(ΔHSI) transgenic mice. DNase I- and XcmI-digested fragments of hepatic chromatin from transgenic mice were mapped using probe Pa. The three XcmI bands on the left autoradiograph from 51-kb hDBP mice correspond to the parental XcmI fragment and the two sub-bands of HSI and HSIII as we have reported previously (22). In the adjacent autoradiograph, the analysis of the hDBP(ΔHSI) transgenic liver chromatin revealed that the parental XcmI fragment was truncated from 3.8 kb to 2.8 kb and HSI was specifically eliminated. HSIII was present in liver chromatin of the DBP(ΔHSI) and hDBP(ΔHSIV,V) (right autoradiograph) transgenic mice and was observed to be composed of two subsignals on this high-resolution mapping gel. (C) Selective inactivation of HSIV and HSV in liver chromatin of the 45-kb hDBP(ΔHSIV,V) transgenic mice. DNase I- and PflFI-digested fragments were mapped using probe Pb. The bands in the left autoradiograph corresponding to the parental PflFI fragment of 13.9 kb and the previously reported HSIV and HSV subfragments are indicated by arrows (22). The WT pattern of HSIV and HSV was maintained in the hDBP(ΔHSI) line. In the hDBP(ΔHSIV,V) line, the size of the parental PflFI fragment was decreased by 6.4 kb as expected and the sub-bands were eliminated. HSIV and HSV were maintained in the hDBP(ΔHSI) transgenic lines (middle autoradiograph). The specific lines studied in panels B and C are indicated below the respective panels.

expression from the single-copy hDBP(ΔHSI) line 2004C was indistinguishable from that of the multicopy lines (Fig. 4). These protein data are concordant with the mRNA expression studies and demonstrated a nonredundant role for the HSIV-HSV region in site-of-integration-independent activation of hDBP transgene. This property fulfills the operational definition of an LCR (31, 32).

Interestingly, there was evidence for sexual dimorphism in the transgene expression in the lines generated with both deletion transgenes (Fig. 4B). The serum levels in all four hDBP(ΔHSI) lines were 27% to 43% lower in adult females than those in littermate males ($P < 0.002$). The serum levels in female hDBP(ΔHSIV,V) mice were also significantly lower than those of male mice ($P < 0.002$), with the exception of line 2017B. The mean serum hDBP levels observed in the adult female mice of the remaining six lines were 30% to 57% of

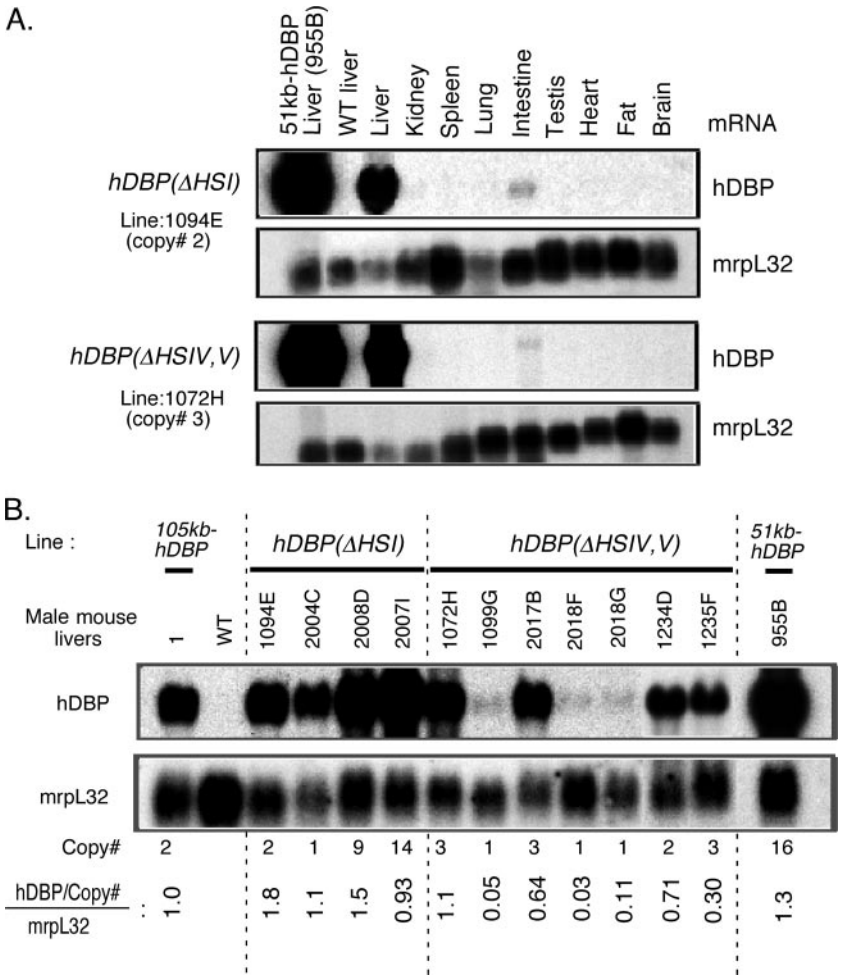

FIG. 3. The HSIV-HSV region is critical to high-level and site-of-integration-independent expression of the hDBP transgene. (A) The liver specificity of hDBP transgene expression is unaffected by deletion of HSI or HSIV-HSV. Total RNAs from various tissues of adult male mice from the two deletion lines hDBP (ΔHSI) line 1094E (transgene copy number 2) and hDBP(ΔHSIV,V) line 1072H (transgene copy number 3) were analyzed. RNAs from the 51-kb hDBP transgenic mouse line 955B (transgene copy number 16) and WT mouse livers served as positive and negative controls (first and second lanes, respectively). The Northern blots were hybridized with an hDBP cDNA fragment and then with a mouse ribosomal protein L32 (mrpL32) cDNA fragment to normalize for RNA loading (indicated at the right). Liver-specific expression of the hDBP(ΔHSI) and hDBP(ΔHSIV,V) transgenes was maintained in both deletion lines. Trace expression was detected in intestinal tissue from both deletion lines. Overall, tissue expression profiles of the hDBP(ΔHSI) and hDBP(ΔHSIV,V) transgenes were consistent with that of the intact 51-kb hDBP transgene (22). (B) Deletion of HSIV-HSV eliminated copy number dependency of hDBP transgene expression. Total RNAs from adult male livers of hDBP(ΔHSI) and hDBP(ΔHSIV,V) transgenic mice were hybridized with an hDBP cDNA probe and then with an mrpL32 cDNA probe as a loading control. Total RNAs from the 105-kb hDBP and 51-kb hDBP transgenic mice (line 1, transgene copy number 2, and line 955B, transgene copy number 16, respectively) were used as positive controls. A representative Northern blot is shown. hDBP mRNA was quantified for each line and normalized to the mrpL32 signal to correct for RNA loading. The normalized hDBP expression value was divided by the transgene copy number, and the ratio for the 105-kb hDBP transgenic line 1 was arbitrarily set to 1.0. The ratios from remaining lines were normalized to the 105-kb hDBP transgenic line 1 and are displayed under the autoradiograph. All quantifications were done by PhosphorImager analysis, and all were in the linear range of detection. The hDBP mRNA levels in the hDBP(ΔHSI) transgenic lines were comparable to those of the 105-kb hDBP line 1 and 51-kb hDBP line 955B and were found to be tightly copy number dependent, varying from 0.93 to 1.8. In contrast, the hDBP mRNA levels in single-copy lines of the hDBP(ΔHSIV,V) lines were much lower, and ratios varied from 0.03 to 1.1. These data indicated that the hDBP(ΔHSIV,V) transgene had lost its copy number dependency.

those in the adult males (data not shown). This sexual dimorphism was not observed in our analyses of the 105-kb hDBP and 51-kb hDBP lines (Fig. 4B). The HS deletions appear to unmask determinants involved in this sexual dimorphism.

Histone acetylation at the hDBP chromatin locus. LCR determinants can target histone-modifying complexes to critical sites during locus activation (14, 48). To characterize elements involved in hDBP activation, we performed ChIP analyses of histone H3 and H4 acetylation across the hDBP gene locus (kb −2.1 to 43.9) (Fig. 5, top, and Table 1). Matched sets of liver and brain chromatin preparations from the same 105-kb hDBP transgenic mice were compared for histone acetylation using six sets of primers along the hDBP locus. All PCR assays were confirmed to be in the linear range by assaying serial dilutions of each DNA sample. Modifications at promoters of the strongly expressed phenylalanine hydroxylase (mPAH) (39)

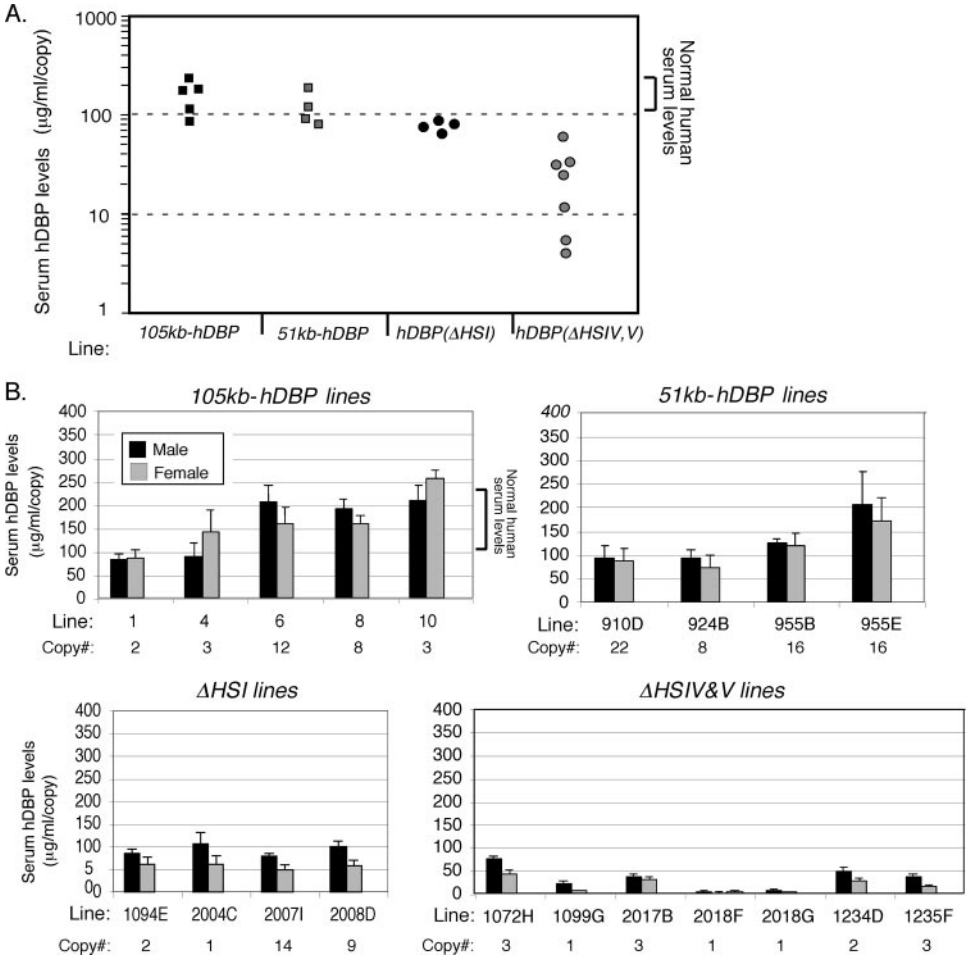

FIG. 4. Quantification of serum hDBP levels in the hDBP(ΔHSI) and hDBP(ΔHSIV,V) mice confirmed the importance of the HSIV-HSV region in establishing robust and consistent levels of gene expression. (A) Mean values of serum hDBP protein per transgene copy number. The RID assay or ELISA was used to quantify levels of serum hDBP. The data are represented on a logarithmic scale. An ELISA was selectively used in the analysis of mice from single-copy lines [hDBP(ΔHSIV,V) lines 1099G, 2018F, and 2018G], because their hDBP levels were very low and could not to be quantified by the less sensitive RID assay. The lines containing the WT transgene lines are represented by rectangles, and the lines carrying the two deletion transgenes are represented by circles. The data from the 105-kb hDBP lines previously reported (22) are displayed to facilitate comparisons. The mean levels of serum hDBP protein per copy number in the hDBP(ΔHSIV,V) lines were significantly decreased compared to the levels in the WT 105-kb hDBP, 51-kb hDBP, and hDBP(ΔHSI) lines ($P < 0.05$), while there was not a statistically significant difference between the hDBP(ΔHSI) and intact 51-kb hDBP lines. (B) Evidence for sexual dimorphism in expression from the two deletion hDBP transgenes. The average values (± standard deviation) in males or females are indicated by black or gray bars, respectively. In all four hDBP(ΔHSI) lines and six hDBP(ΔHSIV,V) lines, with the exception of line 2017B, the hDBP protein levels in females were significantly lower than the levels in males ($P < 0.002$).

and the GAPDH (mGAPDH) genes served as liver-specific and "housekeeping" positive controls, respectively, in each study. Ratios of bound to input DNA at each site in the hDBP locus were normalized to modification at the mGAPDH promoter (defined as 1.0).

The ChIP analyses revealed liver-specific histone H3 acetylation at levels significantly above that in the brain preparations at all six of the tested positions across the hDBP locus (Fig. 5). This modification peaked in the hepatic chromatin within the regions detected by the HSI and HSIV amplimers (Fig. 5, upper histogram). Acetylation at these sites was equivalent to or greater than that of mGAPDH and PAH positive controls. It should be noted that the ChIP assay was carried out on chromatin fragments ranging from 500 to 1,500 bp and that DNA detected by the HSIV amplimer would therefore also reflect modifications at the adjacent HSV. Acetylation of histone H4 generally paralleled histone H3 acetylation, although in general there was a more prominent difference between transgenic hepatic and brain chromatin in the H3 acetylation study. As was the case with H3 acetylation, the most prominent peak of H4 acetylation was observed within the HSIV region in intron 1 (Fig. 5, lower histogram). Compared with brain chromatin, the HSI site, the kb +3.4 site between HSIII and HSIV, and the kb +43.2 site corresponding to HSVI and HSVII were also significantly enriched for acetylated H4 in transgenic hepatic chromatin. ChIP analyses of a second, independent 105-kb hDBP line (line 1, transgene copy number of 2) (22) gave essentially identical results (data not shown).

These acetylated H3 and H4 studies revealed that the promoter-intron 1 region encompassing HSI and HSIV (probably

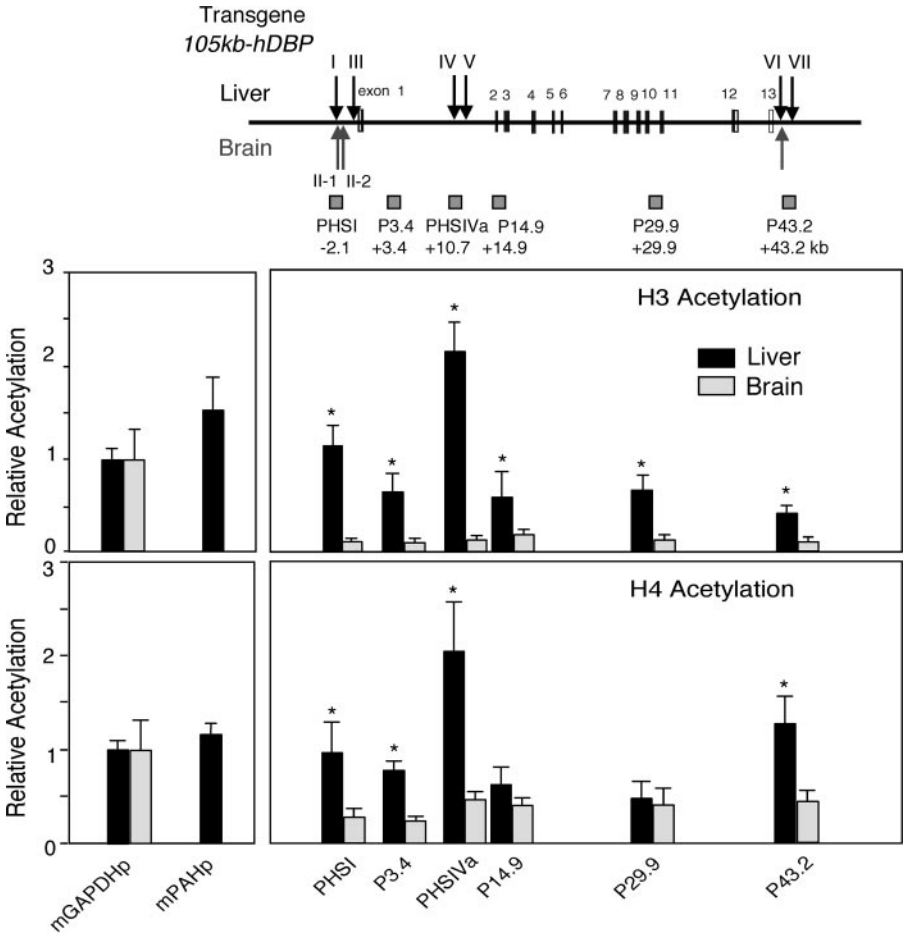

FIG. 5. A peak of histone acetylation at the hDBP locus in liver chromatin comapped to the liver-specific HSIV region in intron 1. A physical map of the hDBP gene with the full set of DNase I HSs that were previously identified by analysis of liver and brain chromatin from the 105-kb hDBP transgenic mice (22) is shown. Vertical arrows indicate the positions of the HS (downward, liver; upward, brain). Positions of the primers and hybridization probes for the ChIP assays are indicated by the labeled gray rectangles below the map. The two panels below summarize the relative levels of acetylated histones H3 and H4 across the hDBP locus at the positions indicated on the map, as determined by ChIP of liver (black bars) or brain (gray bars) chromatin. Samples were obtained from 105-kb hDBP transgenic mouse line 6 (transgene copy number 12). Relative acetylation values were determined and normalized to that of the constitutively active endogenous mGAPDH promoter (arbitrarily defined as 1.0). The values at the mPAH promoter (a positive control) in liver chromatin are also shown. Error bars reflect the standard deviation of the average signal obtained from at least three PCR assays in two independent ChIP experiments. *P* values for comparisons between liver and brain data were determined by Student's *t* test. *, $P < 0.01$.

including HSV), as well as the HSVI and HSVII regions near the poly(A) site, were highly acetylated in liver. The highest levels of modification mapped to the region of intron 1. These data are consistent with a model in which determinant(s) in this region are critical to activation of the hDBP locus.

Interaction of the hepatocyte-enriched transcription factor C/EBPα with HSIV and its role in hDBP gene activation. Based on the functional and chromatin modification studies summarized above, we next focused our attention on the structure and function of the intron 1 chromatin determinants. Alignment of the region encompassing HSIV (kb +10.3 to +10.9 in intron 1) with the corresponding regions in the mouse and rat genomes revealed a central 275-bp region (kb +10.67 to +10.95) with 63% sequence similarity among the three species (Fig. 6A). This region was found to contain predicted binding sites for several liver-enriched transcription factors. Of particular note was a conserved array of putative C/EBP binding sites. EMSA of this conserved DNA segment was carried out with nuclear extracts prepared from primary mouse liver and from two well-characterized human hepatocellular carcinoma cell lines, HepG2 and Hep3B. Comparison of the two hepatic cell lines was potentially informative because hDBP is expressed in Hep3B cells, but not in HepG2 cells (19, 29) (Fig. 6B), while the two DBP paralogs, albumin and α-fetoprotein, are expressed in both cell lines (29, 30, 38). EMSA probes corresponding to the two most highly conserved C/EBP binding sites (f1 and f2) (core and matrix similarities of >0.85 [Fig. 6A]) assembled robust complexes in all three extracts. However, the majority of C/EBP complexes formed with primary liver and Hep3B extracts were recognized and supershifted with C/EBPα antibodies, whereas a reciprocal specificity for binding by C/EBPβ was observed in the HepG2 cell extract (Fig. 6C). The comparison of hDBP expression patterns with the EMSA studies points to a functional linkage between the

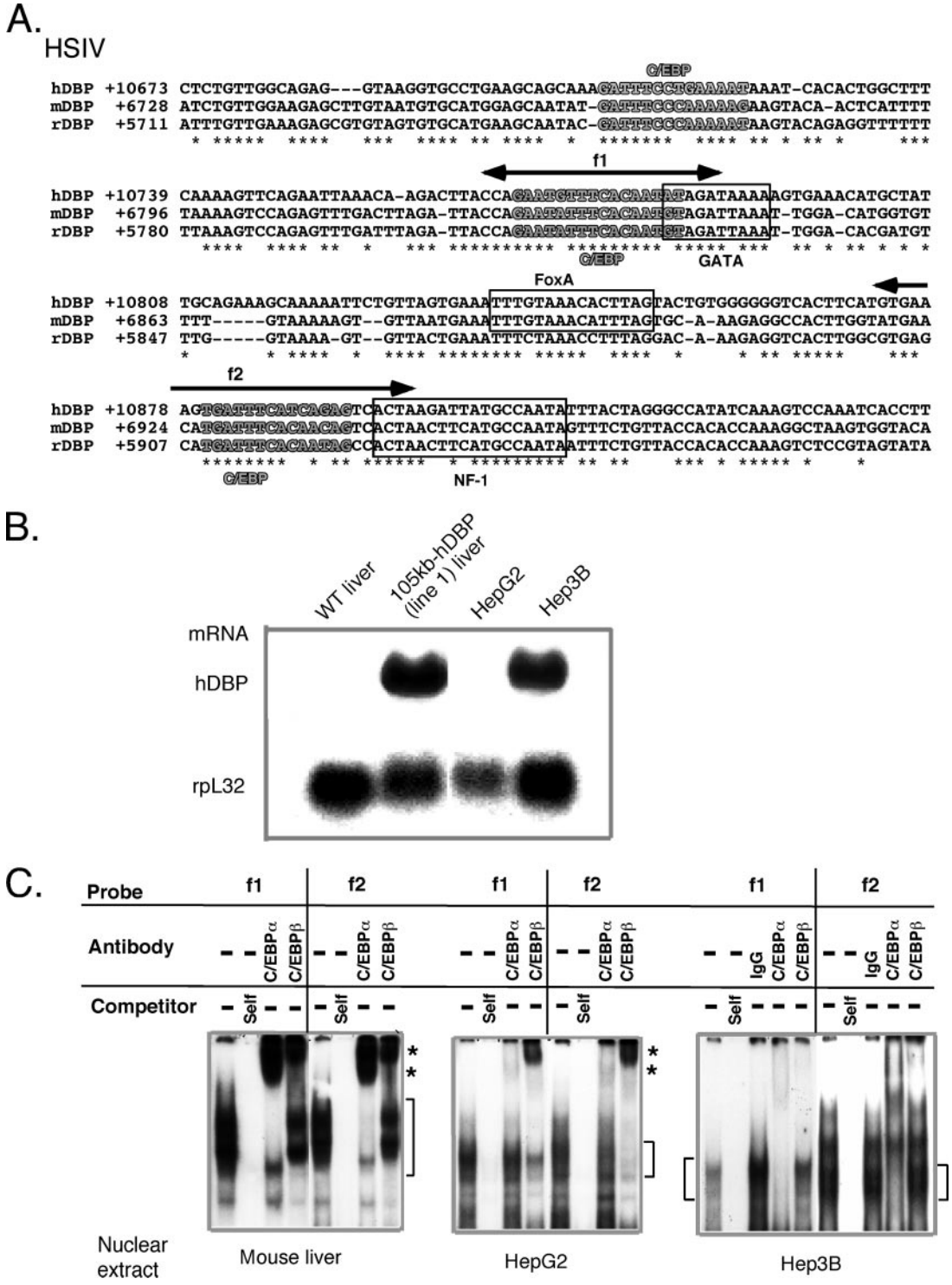

FIG. 6. EMSAs indicated that predicted C/EBP binding sites in HSIV can associate with C/EBP. (A) Alignment of sequences within the HSIV region. Sequences encompassing HSIV in human genomic DNA were aligned with the corresponding sequences in intron 1 of the mouse and rat *DBP* genes. The segments corresponding to +10673 to +10947 in intron 1 of the hDBP gene have an overall 63% sequence similarity to the other two species. Bases conserved in all three species are indicated (asterisks). The numbering of the sequences for each of the three species begins with the site of transcription initiation that is defined as 1. The segment shown contains the consensus binding sites for several transcription factors, including C/EBP, FoxA (HNF3), NF-1, and GATA, all known transcriptional regulators for a number of liver-specific genes (program Match public version 1.0). The C/EBP consensus sites are highlighted in large gray letters. The consensus binding sites for FoxA, NF-1, and GATA are each indicated by the labeled boxes. Probes f1 and f2 (double-headed arrows) contain the second and third predicted and most highly conserved C/EBP binding sites, respectively. These two probes were used for EMSA (C). (B) hDBP was robustly expressed in mouse liver and Hep3B cells but not in HepG2 cells. The autoradiograph of a Northern blot is shown. Total RNA from the livers of a WT mouse and a 105-kb hDBP transgenic mouse (line 1; two copies), HepG2 cells, and Hep3B cells were analyzed. The two probes used are indicated to the left of the autoradiograph; hybridization

observed C/EBPα binding at HSIV and activation of the hDBP locus. In contrast, C/EBPβ bound to the f1 and f2 C/EBP sites in both expressing Hep3B cells and silent HepG2 cells, suggesting that it may have no specific role in *DBP* expression.

A role for C/EBPα in *DBP* activation was assessed in cell culture. As noted above, hDBP is robustly expressed in native Hep3B cells (Fig. 6B) and C/EBPα in Hep3B nuclear extracts binds to sequences within the conserved HSIV region (Fig. 6C). Hep3B cells were depleted of C/EBPα mRNA by treatment with C/EBPα siRNA (Fig. 7A). Northern blot analyses revealed depletion of hDBP mRNA in cells treated with C/EBPα siRNA to 50% of the level in cells treated with a control lamin A/C siRNA (Fig. 7B shows a representative of two Northern blots with consistent results). Comparison to a mock transfection control gave an equivalent but slightly greater level of repression. Western blot analysis confirmed a decrease of hDBP protein expression in cells depleted of C/EBPα (Fig. 7C). These results support a contribution of C/EBPα to hDBP gene activation.

The role of C/EBPα in *DBP* expression was further assessed in vivo. mDBP mRNA was quantified and compared in livers of mice null for *C/EBP*α (50) and *C/EBP*β (18) and in their WT littermates. The level of mDBP mRNA in the livers of *C/EBP*α-null mice normalized to 18S rRNA was approximately 50% of the level in WT mouse liver and in *C/EBP*α-heterozygote littermates (Fig. 8A). In contrast, there was no repression of mDBP mRNA in livers of *C/EBP*β-null mice (Fig. 8B). The conservation of C/EBPα binding sites at the HSIV region in both humans and rodents (mouse and rat) and the parallel impact of C/EBPα in hepatic cells of human (HepG3) and mouse origins support a conserved role for these C/EBP binding sites in *DBP* activation.

We next assessed the in vivo occupancy of C/EBP sites within the hDBP locus. Hepatic chromatin from the 105-kb hDBP transgenic mice was cross-linked, fragmented, and incubated with antibodies specific to C/EBPα or C/EBPβ. The hDBP locus was scanned using five sets of primers (Fig. 9A and Table 1). The ratio of signal intensities at each site was normalized to binding to intron 2 of the gene coding for mouse testicular cell adhesion molecule 1 (TCAM1), a testis-specific gene (expression defined as 1.0). The study revealed strong and specific association of C/EBPα and C/EBPβ with HSI and HSIV; levels of binding at the other three sites surveyed, representing the DBP core promoter, the proximal region of intron 1, and intron 10, were at background levels. Enrichment for C/EBPβ was equivalent at HSI and HSIV, whereas that for C/EBPα was slightly more pronounced at HSIV than at HSI. The association of C/EBP isoforms with HSIV was consistent with the identified array of conserved C/EBP binding sites in this region (Fig. 6). Binding at HSI was consistent with the presence of two conserved C/EBP consensus sites in the region 2 kb 5′ to the hDBP promoter (data not shown). However, not all predicted C/EBP sites were occupied in vivo because the region of the hDBP core promoter containing a conserved

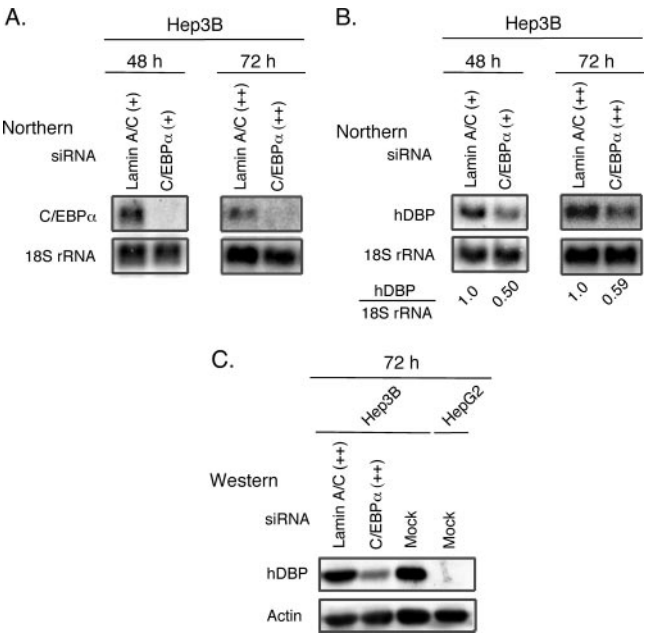

FIG. 7. siRNA-mediated depletion of CEBPα in Hep3B cells resulted in decreased expression of hDBP. Hep3B cells were treated with lamin A/C siRNA (control) or C/EBPα siRNAs. Total RNAs (5 μg per lane) isolated from the indicated cells were subjected to Northern analyses. Each Northern blot was hybridized with the hDBP cDNA probe or the hC/EBPα cDNA probe. The blots were rehybridized with an 18S rRNA oligonucleotide probe (Table 1) (41) to normalize for RNA loading. Levels of hDBP mRNA in cells treated with C/EBPα siRNA were normalized to an arbitrary level of 1.0 assigned to that in the lamin A/C siRNA-treated cells (a control for the siRNA transfection). Cells were harvested at 48 h after a single siRNA transfection (left panels in panels A and B). An additional siRNA transfection was performed on the cells at 48 h. These cells were then harvested for analysis at 72 h as indicated: +, single transfection; ++, double transfections (right panels in panels A and B and first two lanes in panel C). In both cases, C/EBPα mRNA was essentially eliminated by the siRNA treatment (A) and the levels of hDBP mRNA in these cells were 50 to ~60% of those in lamin A/C siRNA-treated control cells (B). The effect of C/EBPα knockdown was assessed by determining hDBP protein levels by Western blotting. Total protein in Hep3B or HepG2 cells (mock) served as a positive or negative control for hDBP protein expression, respectively. Actin levels in each sample served as loading controls. hDBP protein levels in Hep3B cells treated with C/EBPα siRNAs were decreased compared with that in control cells treated with lamin A/C siRNA (C). Similar results were obtained in two independent experiments (not shown).

with a mouse ribosomal protein L32 (rpL32) cDNA probe was used to normalize results for loading. (C) EMSAs confirmed in vitro binding to two highly conserved C/EBP sites within the HSIV region. ^{32}P-labeled double-stranded f1or f2 probes (A) containing the two highly conserved C/EBP binding site from the HSIV region were individually incubated with nuclear extracts from mouse liver, HepG2 cells, or Hep3B cells. Competition studies were carried out with a 200-fold molar excess of probe ("Self"). Antibody supershift studies were done with rabbit polyclonal antibodies specific for C/EBPα or C/EBPβ and controlled with normal rabbit IgG. Binding reaction mixtures were electrophoresed on a nondenaturing 5% polyacrylamide gel. The gels were dried and exposed to X-ray film. DNA-protein complexes, defined by self-competition sensitivity, are indicated by brackets. Supershifted complexes generated with the indicated antibodies are denoted with asterisks.

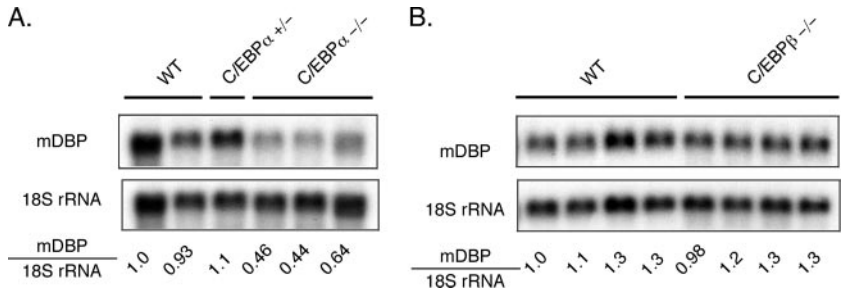

FIG. 8. Levels of mDBP mRNA were selectively decreased in the livers of *C/EBP*α-null mice. The autoradiographs show two representative Northern blots of total liver RNAs (5 μg per lane) isolated from wild-type, *C/EBP*$\alpha^{+/-}$, or *C/EBP*$\alpha^{-/-}$ littermates (A) and from wild-type or *C/EBP*$\beta^{-/-}$ littermates (B). The Northern blots were hybridized with a probe corresponding to a 290-bp sequence of the mDBP gene extending from exon 5 to exon 7. The blots were rehybridized with an 18S rRNA oligonucleotide probe (Table 1) (41) to normalize for RNA loading in each lane. Levels of mDBP mRNA in each sample were normalized to an arbitrary level of 1.0 assigned to the WT sample (left lane); each normalized value is indicated under the respective lane in the autoradiographs.

C/EBP site (at bp −130) (data not shown) was not enriched for C/EBP in our ChIP study (HSIII amplimer [Fig. 9B]).

The evidence for in vivo occupancy of C/EBPα at HSIV supports a functional role for the corresponding complex or complexes in hDBP activation. Although C/EBPα also bound to the HSI region, the minimal impact of HSI deletion on hDBP transgene expression suggested that this interaction is not critical. Similarly, C/EBPβ binding at HSIV was not matched by evidence for a functional impact because deletion of *C/EBP*β in mice failed to alter mouse *DBP* expression (Fig. 8).

ChIP survey of the hDBP locus demonstrated the involvement of HNF1α at HSIII in the proximal promoter. Neither HSI, HSIV, nor HSV appeared to dictate liver restriction of hDBP expression (Fig. 3A). To explore the basis for this liver specificity, we focused on HSIII and in particular on the interaction of the liver-specific factor HNF1 with this promoter region. We had previously identified three functional HNF1-binding sites within the promoter-proximal region of the rat *DBP* (rDBP) gene: segment A at bp −141 to −43; segment B at bp −254 to −140; and a more distal segment, F-2, at bp −1844 to −1621 (44). All three sites enhance rDBP promoter function when tested in reporter-based cell transfection assays, and HNF1α plays a predominant role in this process (44). The two HNF1-binding sites in segments A and B of the rDBP promoter are highly conserved at the human locus (22). We performed ChIP analysis of 105-kb hDBP transgenic locus to determine whether HNF1 interacted with the HSIII site in vivo. Antibodies to the two major HNF1 isoforms, HNF1α and HNF1β, were used in the study. The results demonstrated that HNF1α is selectively and strongly associated with the HSIII site in vivo (Fig. 9C). This selective enrichment for HNF1α at HSIII of the hDBP proximal promoter is consistent with the previously documented positive transcriptional control of HNF1α at the rDBP promoter.

DISCUSSION

In a previous report, we demonstrated that the hepatic expression of an hDBP transgene containing minimal 5′- and 3′-flanking sequences is robust, liver specific, and copy number dependent. Furthermore, the chromatin locus associated with this 51-kb hDBP transgene assembles all five of the liver-specific HSs (HSI, HSIII, HSIV, HSV, and HSVII) that were initially mapped in a more extensive hDBP transgene (22). Based on these findings, we postulated that one or more of these HSs retained in the 51-kb hDBP contain determinants critical to the establishment of a fully autonomous chromatin domain that can support consistent hepatic activation of hDBP. These characteristics would fulfill the operational definition of an hDBP LCR (22).

To elucidate the functional components of this hDBP LCR, we focused our initial efforts on HSI in the 5′-flanking region and on HSIV-HSV within intron 1. The functional importance of these sites was tested by corresponding deletions from the 51-kb hDBP transgene. Two transgenes were generated and tested: the first lacked HSI [hDBP(ΔHSI)], and the second lacked both HSIV and HSV [hDBP(ΔHSIV,V)]. Expression of hDBP from these deletion transgenes was compared to that of the intact 51-kb hDBP transgene from which they were derived. Three major observations resulted from these studies. First, liver specificity of hDBP expression was maintained in the absence of HSI and in the absence of HSIV and HSV. This led us to consider whether HSIII, which maps to the *DBP* proximal promoter, might constitute a critical determinant for tissue-specific expression of hDBP (see below). Second, HSI does not constitute a critical element of the hDBP LCR. This conclusion was supported by the observation that expression in four hDBP(ΔHSI) lines was maintained at the same level and in the same tight copy number dependence as that observed for the intact 51-kb hDBP. Third, the region of intron 1 containing HSIV and HSV is critical to the establishment of a fully productive hDBP chromatin locus. Deletion of the region rendered the hDBP transgene sensitive to position effects and repressed the overall expression level when compared to the intact 51-kb hDBP and the 50-kb hDBP(ΔHSI) transgenes. In particular, the hDBP protein levels in single-copy hDBP (ΔHSIV,V) lines were 3 to 11% of the mean level in the intact 51-kb hDBP lines. The impact of the HSIV-HSV deletion appeared to represent a direct effect because the other HSs were retained at the hDBP(ΔHSIV,V) locus. We note that the intronic HSIV-HSV region is separated from the target hDBP promoter by a significant distance, 10 to 12 kb. Thus, its ability to overcome position dependence and maintain robust expression of the target hDBP promoter is exerted in a long-range

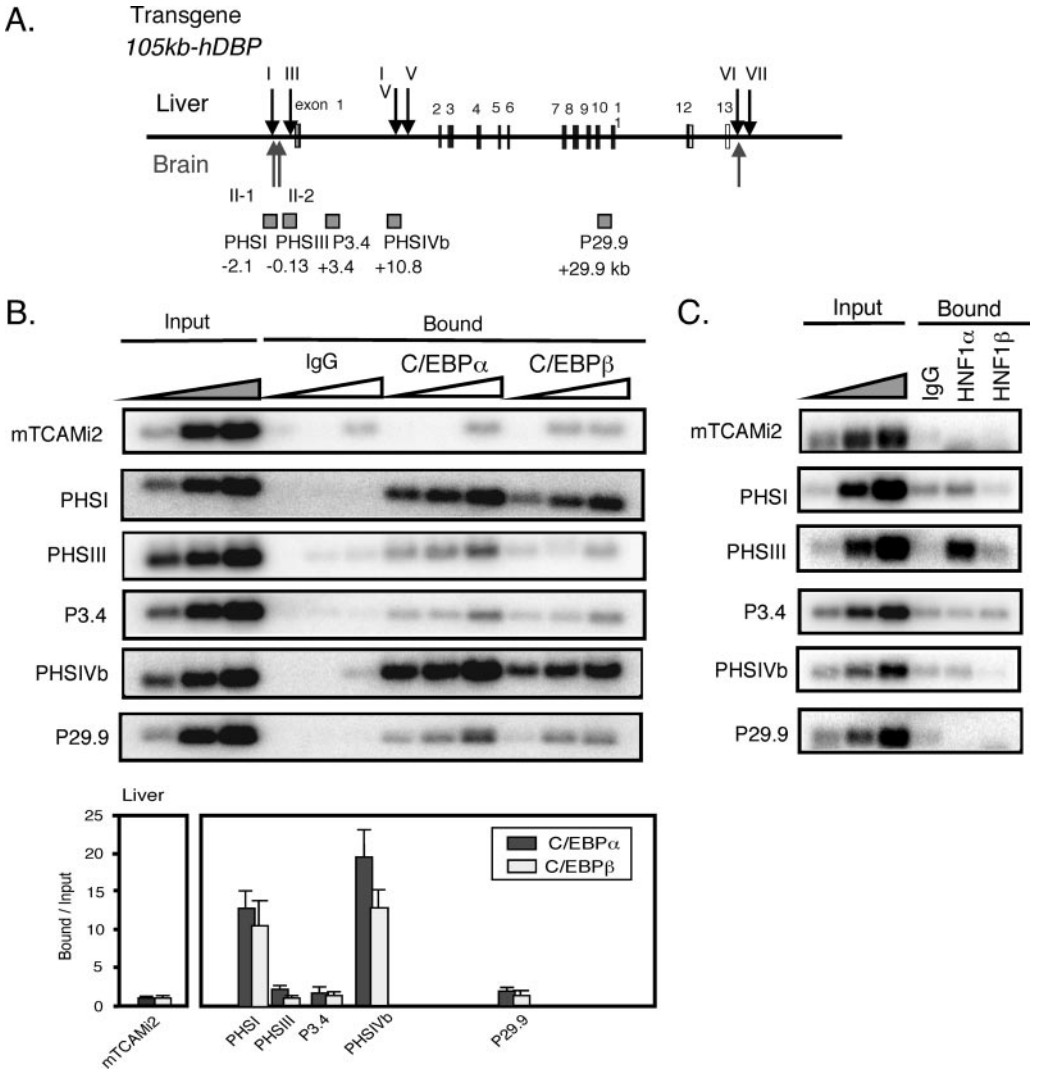

FIG. 9. In vivo occupancy of C/EBPα and C/EBPβ at HSIV and HNF1α at the hDBP promoter in transgenic liver chromatin. (A) Physical map of the hDBP gene locus. The map is as described in the legend to Fig. 5, but with the positions of the primers and hybridization probes for this ChIP assay indicated by the labeled gray rectangles below the map. (B) ChIP survey revealed association of both C/EBPα and C/EBPβ at the HSIV region in intron 1 and at the HSI region. ChIP analysis was performed using liver chromatin from the 105-kb hDBP transgenic mice and C/EBPα and C/EBPβ antibodies. The autoradiographs are representative Southern hybridizations of the PCR-amplified fragments from C/EBP ChIP. The wedges indicate serially increasing DNA concentrations of each of the input (gray) and bound (white) DNA samples showing the linearity of the PCR. The locations of each of the five amplicons used in the ChIP assays of the 105-kb hDBP transgene are indicated to the left of the autoradiographs. The relative values of bound to input signals were determined and normalized to that at the endogenous mouse testis-specific *TCAM* gene intron 2 (mTCAMi2; negative control), which was defined as 1.0. The normalized values were plotted on the histogram (dark bars, C/EBPα; light bars, C/EBPβ). Error bars reflect the standard deviation of the average signal obtained from at least three PCR assays in two independent ChIP experiments. (C) Selective association of HNF1α at the HSIII site in the hDBP proximal promoter. ChIP analysis of HNF1α and HNF1β in liver chromatin from the 105-kb hDBP transgenic mice was performed as described in panel B. The autoradiographs are representative Southern hybridizations of the PCR-amplified fragments from the two HNF1 ChIPs (three PCR assays in two independent ChIP experiments). Sequential dilutions of the input chromatin samples are shown along with a single linear-range dilution of the bound fraction.

fashion. Such long-range effects are characteristic of LCR determinants (9).

Histone modifications can alter histone-DNA packaging and establish specialized binding sites for protein complexes involved in subsequent steps in gene control. Core histone H3 and H4 acetylation, an extensively studied example of such modification, is generally correlated with transcriptional activity at promoters, enhancers, and a number of LCR elements (reviewed in references 15, 23, and 32). Our mapping study of histone acetylation revealed that the hDBP locus is encompassed in an acetylated chromatin domain. Within this domain, there are prominent peaks of H3 and H4 acetylation mapping to the HSIV region. These results are consistent with a prominent role of HSIV as a liver-specific LCR component, possibly as a site for histone acetyltransferase (HAT) complex recruitment. The HSI region is also enriched for H3 acetylation, but functional testing failed to link this to an essential activity. The HSVII region, located immediately 3′ to the poly(A) site, is of

note in that it is selectively enriched for acetylation of histone H4. The model of the "histone code" proposes that different patterns of acetylation can mediate distinct functions (24). The distinct acetylation profile of HSVII and its position flanking the 3′ end of the gene suggest a possible role as a boundary element that might limit the extent of the autonomous chromatin domain. Thus, the various HSs in the hDBP locus may mediate distinct functions or relate in ways not adequately reflected in our transgenic models. What is most clear from these data is the central role of the HSIV in hDBP gene activation.

High-resolution DNase I mapping of the hDBP transgene locus has previously revealed that HSIV is composed of three subsites (22). This region contains an array of three conserved C/EBP binding consensus sites. EMSA studies revealed that C/EBPα binds more abundantly to these sites than C/EBPβ when assessed and compared in extracts of hDBP-expressing and -nonexpressing cells (Fig. 6). A ChIP survey of the hDBP gene locus in the transgenic liver chromatin confirmed in vivo occupancy of C/EBP at HSIV and showed that C/EBPα binding was significantly more abundant than C/EBPβ binding at this site. ChIP analysis also revealed the involvement of C/EBP at the HSI site, although there was significantly less C/EBPα binding than at HSIV (Fig. 9). The siRNA knockdown study in hDBP-expressing hepatocellular Hep3B carcinoma cells and analysis of *C/EBP*α- and *C/EBP*β-knockout mice demonstrated a nonredundant role for the C/EBPα isoform for full levels of *DBP* activation (Fig. 7 and 8). In contrast, we found no specific role for C/EBPβ.

HNF1 is a homeodomain-containing protein that is expressed as two isoforms, HNF1α and HNF1β. HSIII is located between the two predicted HNF1-binding sites, A and B, in the DBP promoter. The functional importance of these sites in promoting DBP transcription was initially revealed by in vitro and cell transfection analyses of the rat *DBP* proximal promoter (44). The B-binding site, located 254 to 140 bp 5′ to the transcription start site, was the main mediator of both HNF1α enhancing activity and for a competing HNF1β *trans*-dominant repressive activity (44). The present ChIP analysis demonstrated that HNF1α, but not HNF1β, selectively bound the HSIII site in the core promoter of the hDBP gene in vivo (Fig. 9C). HNF1α has been shown by others to recruit the HATs CBP, p300/CBP-associated factor (P/CAF), and Serc-1. These HNF1 targeted interactions contribute to HNF1α-dependent transcriptional enhancement in functional assays both in vitro and in vivo (39, 45, 47). For example, differentiation-induced activation of the human α1-antitrypsin gene is initiated by recruitment of HNF1α to the packed nucleosomes at its proximal promoter along with general transcription factors, TBP and TFIIB. PolII then joins the preinitiation complex, and another activator, HNF4α, and HAT coactivators are recruited. These associations result in subsequent histone acetylation and nucleosome remodeling (46). Selective association of HNF1α at the HSIII site suggested that HNF1α might contribute to local promoter assembly for hDBP transcriptional activation by recruiting HAT(s) to the proximal promoter and remodeling local chromatin architecture. The functional importance of HNF1α in DBP expression has been previously demonstrated by the observation of a 50% decrease of *DBP* mRNA levels in the livers of the *HNF1*α-null (*HNF1*$\alpha^{-/-}$) mice compared to WT littermates (44). This impact is similar to the decrease that was observed in *C/EBP*α-null (*C/EBP*$\alpha^{-/-}$) mouse livers and in C/EBPα siRNA-treated Hep3B cells (Fig. 7 and 8). These observations lead us to suggest that both HNF1α and C/EBPα contribute in a positive manner to expression of the hDBP gene by binding the HSIII and HSIV sites, respectively. It is reasonable to consider the possibility that HNF-1 bound to HSIII may be directly involved in the liver restriction of DBP expression.

The sexual dimorphism detected in the expression of hDBP from the two deletion transgenes (Fig. 4B) was unexpected. The hDBP levels expressed in females were lower than those in males in all four hDBP(ΔHSI) and six of seven hDBP (ΔHSIV,V) transgenic lines (Fig. 4B). In prior studies of the intact 51-kb hDBP and the more extended 105-kb hDBP transgenic lines, we have failed to detect a similar phenomenon. The mechanistic basis for the unmasking of this effect, documented in both sets of transgene deletions, remains to be explored.

It should be emphasized that HSIV is closely flanked within intron 1 by HSV (at kb +10.3 to 10.9 and +12.2, respectively). Emphasis in the present study has been on HSIV due to its conserved noncoding sequences that contain the array of C/EBP binding sites and the linkages between binding at these sites and DBP gene activation. The limits of resolution of the ChIP assays in this study do not in any way eliminate contributions of HSV to these processes. Thus, the function of HSV, either as a facilitator of HSIV activity or as an independent determinant and component of the LCR, remains open to further study.

The HSs in intron 1 are separated from the hDBP promoter by 10 to 12 kb. These sites are able to overcome position effects at random insertion sites in the host mouse chromatin. They also establish an environment that sustains consistent and robust expression equivalent to that of the hDBP gene in its native genomic setting. How this long-range control of the hDBP promoter by these elements is mediated remains to be determined. Several models for long-range activation have been explored in the literature. These include looping, tracking, and linking. Combinations of facilitated tracking and looping have been proposed for long-distance interaction of LCR elements (enhancers) and promoters (5, 9, 32). Although a peak of histone acetylation maps to HSIV, the 13-kb region encompassing HSI, HSIII, and HSIV (probably including HSV) exists in a domain of acetylated histones H3 and H4. Such a continuous domain of modification might be most consistent with a tracking model for this long-distance interaction. However, looping and direct contact between the intronic elements and the promoter are not ruled out by these data and further epigenetic mapping and structural characterization of the active locus should shed further light on this problem.

Several peculiar aspects of hDBP transcriptional control are highlighted by the present study. As noted above, the hDBP gene is a part of a multigene locus that includes *ALB*, *AFP*, and α-*ALB*, all of which are expressed predominantly in liver, and are activated with developmentally distinct schedules. While the *ALB*, *AFP*, and α-*ALB* genes are closely juxtaposed to each other, hDBP, is located more than a megabase upstream (43). Thus, regulation of hDBP might reflect qualities of a single, isolated gene and of a multigene family. It is now clear that

despite the common evolutionary origins of all four of these genes and the maintenance of genetic linkage among them, the hDBP gene is regulated in an autonomous fashion. This autonomous regulation of a single member of a multigene family contrasts markedly with the situation in two other intensively studied clusters, those containing the human β-globin and growth hormone genes. The coregulation and developmental coordination of five linked genes in each of these two gene clusters are under the control of single multicomponent LCR units (23). There is at present no evidence to suggest that the hDBP LCR is involved in coordinated regulation of *ALB*, *AFP*, and α-*ALB*. Also, the LCRs of the human β-globin and GH clusters, and most other defined clusters, are located external to, and remote from, the target genes. In contrast, the critical HSIV element of the hDBP LCR is internal to the gene unit. The ability of the hDBP(ΔHSI) transgene, containing minimal 5′- and 3′-flanking sequences (1.3 and 6.5 kb, respectively), to establish copy-number-dependent expression, tissue specificity, and appropriate levels of expression is consistent with the major role of the intronic HSIV. We also note that, contrary to most current models of genome organization, elements that protect a transgene from site-of-integration effects do not need to be physically located at external "boundary" positions. Instead an element, such as the hDBP HSIV, may "insulate" the locus by exerting long-range controls over chromatin structure and conformation. Future studies of the hDBP LCR that focus on deciphering the mechanistic roles of long-range alterations in chromatin structure are therefore likely to be of general interest in advancing the understanding of transcriptional regulation in metazoan organisms.

ACKNOWLEDGMENTS

We thank Jean Richa and the Transgenic and Chimeric Mouse Core of the University of Pennsylvania and the Center for Molecular Studies in Digestive and Liver Diseases (NIH P30 DK50306) for the generation of transgenic lines and Chris Laing in our laboratory who developed the ELISA for mouse serum DBP. We are also grateful to Philip Phuc Le, Klaus Kaestner, and Linda Greenbaum for liver RNA samples from the *C/EBP*α- and *C/EBP*β-null mice.

This study was supported by grant NIH R01 GM32035 (N.E.C. and S.A.L.).

REFERENCES

1. **Allan, C. M., S. Taylor, and J. M. Taylor.** 1997. Two hepatic enhancers, HCR.1 and HCR.2, coordinate the liver expression of the entire human apolipoprotein E/C-I/C-IV/C-II gene cluster. J. Biol. Chem. **272:**29113–29119.
2. **Belanger, L., S. Roy, and D. Allard.** 1994. New albumin gene 3′ adjacent to alpha 1-fetoprotein locus. J. Biol. Chem. **269:**5481–5484.
3. **Boese, Q., D. Leake, A. Reynolds, S. Read, S. A. Scaringe, W. S. Marshall, and A. Khvorova.** 2005. Mechanistic insights aid computational short interfering RNA design. Methods Enzymol. **392:**73–96.
4. **Boren, J., I. Lee, M. J. Callow, E. M. Rubin, and T. L. Innerarity.** 1996. A simple and efficient method for making site-directed mutants, deletions, and fusions of large DNA such as P1 and BAC clones. Genome Res. **6:**1123–1130.
5. **Bulger, M., and M. Groudine.** 1999. Looping versus linking: toward a model for long-distance gene activation. Genes Dev. **13:**2465–2477.
6. **Cooke, N. E., and E. V. David.** 1985. Serum vitamin D-binding protein is a third member of the albumin and a-fetoprotein gene family. J. Clin. Investig. **76:**2420–2424.
7. **Cooke, N. E., and J. G. Haddad.** 1995. Vitamin D-binding protein (Gc-globulin). Endocr. Rev. **4:**125–128.
8. **Cooke, N. E., and J. G. Haddad.** 1997. Vitamin D, p. 87–101. *In* D. Feldman, F. H. Glorieux, and J. W. Pike (ed.), Vitamin D. Academic Press, Orlando, FL.
9. **Dean, A.** 2006. On a chromosome far, far away: LCRs and gene expression. Trends Genet. **22:**38–45.
10. **Dixon, T. M., K. W. Daniel, S. R. Farmer, and S. Collins.** 2001. CCAAT/enhancer-binding protein alpha is required for transcription of the beta 3-adrenergic receptor gene during adipogenesis. J. Biol. Chem. **276:**722–728.
11. **Duong, D. T., M. E. Waltner-Law, R. Sears, L. Sealy, and D. K. Granner.** 2002. Insulin inhibits hepatocellular glucose production by utilizing liver-enriched transcriptional inhibitory protein to disrupt the association of CREB-binding protein and RNA polymerase II with the phosphoenolpyruvate carboxykinase gene promoter. J. Biol. Chem. **277:**32234–32242.
12. **Dyer, R. B., and N. K. Herzog.** 1995. Isolation of intact nuclei for nuclear extract preparation from a fragile B-lymphocyte cell line. BioTechniques **19:**192–195.
13. **Ferrin, L. J., and R. D. Camerini-Otero.** 1991. Selective cleavage of human DNA: RecA-assisted restriction endonuclease (RARE) cleavage. Science **254:**1494–1497.
14. **Fischle, W., Y. Wang, and C. D. Allis.** 2003. Histone and chromatin cross-talk. Curr. Opin. Cell Biol. **15:**172–183.
15. **Forsberg, C. E., and E. H. Bresnick.** 2001. Histone acetylation beyond promoters: long-range acetylation patterns in the chromatin world. Bioessays **23:**820–830.
16. **Gomme, P. T., and J. Bertolini.** 2004. Therapeutic potential of vitamin D-binding protein. Trends Biotechnol. **22:**340–345.
17. **Gorski, K., M. Carneiro, and U. Schibler.** 1986. Tissue-specific in vitro transcription from the mouse albumin promoter. Cell **47:**767–776.
18. **Greenbaum, L. E., W. Li, D. E. Cressman, Y. Peng, G. Ciliberto, V. Poli, and R. Taub.** 1998. CCAAT enhancer-binding protein beta is required for normal hepatocyte proliferation in mice after partial hepatectomy. J. Clin. Investig. **102:**996–1007.
19. **Guha, C., M. Osawa, P. A. Werner, R. M. Galbraith, and G. V. Paddock.** 1995. Regulation of human Gc (vitamin D-binding) protein levels: hormonal and cytokine control of gene expression in vitro. Hepatology **21:**1675–1881.
20. **Haddad, J. G., K. D. Harper, M. Guoth, G. G. Pietra, and J. W. Sanger.** 1990. Angiopathic consequences of saturating the plasma scavenger system for actin. Proc. Natl. Acad. Sci. USA **87:**1381–1385.
21. **Hebbes, T. R., A. L. Clayton, A. W. Thorne, and C. Crane-Robinson.** 1994. Core histone hyperacetylation co-maps with generalized DNase I sensitivity in the chicken β-globin chromosomal domain. EMBO J. **13:**1823–1830.
22. **Hiroki, T., Y. H. Song, S. A. Liebhaber, and N. E. Cooke.** 2006. The human vitamin D-binding protein gene contains locus control determinants sufficient for autonomous activation in hepatic chromatin. Nucleic Acids Res. **34:**2154–2165.
23. **Ho, Y., S. A. Liebhaber, and N. E. Cooke.** 2004. Activation of the human GH gene cluster: roles for targeted chromatin modification. Trends Endocrinol. Metab. **5:**40–45.
24. **Jenuwein, T., and C. D. Allis.** 2001. Translating the histone code. Science **293:**1074–1080.
25. **Kajiyama, Y., J. Tian, and J. Locker.** 2006. Characterization of distant enhancers and promoters in the albumin-alpha-fetoprotein locus during active and silenced expression. J. Biol. Chem. **281:**30122–30131.
26. **Kalkunte, S., L. Brard, C. O. Granai, and N. Swamy.** 2005. Inhibition of angiogenesis by vitamin D-binding protein: characterization of anti-endothelial activity of DBP-maf. Angiogenesis **8:**349–360.
27. **Kimura, A. P., S. A. Liebhaber, and N. E. Cooke.** 2004. Epigenetic modifications at the human growth hormone locus predict distinct roles for histone acetylation and methylation in placental gene activation. Mol. Endocrinol. **18:**1018–1032.
28. **Kisker, O., S. Onizuka, C. M. Becker, M. Fannon, E. Flynn, R. D'Amato, B. Zetter, J. Folkman, R. Ray, N. Swamy, and S. Pirie-Shepherd.** 2003. Vitamin D binding protein-macrophage activating factor (DBP-maf) inhibits angiogenesis and tumor growth in mice. Neoplasia **5:**32–40.
29. **Knowles, B. B., C. C. Howe, and D. P. Aden.** 1980. Human hepatocellular carcinoma cell lines secrete the major plasma proteins and hepatitis B surface antigen. Science **209:**497–499.
30. **Kobsel, N., and G. Ramadori.** 1994. Human hepatoma cells synthesize and secrete lysozyme: modulation by cytokines. Hepatology **19:**1182–1188.
31. **Li, Q., S. Harju, and K. R. Peterson.** 1999. Locus control regions. Trends Genet. **15:**403–408.
32. **Li, Q., K. R. Peterson, X. Fang, and G. Stamatoyannopoulos.** 2002. Locus control regions. Blood **100:**3077–3086.
33. **Liebhaber, S. A., Z. Wang, F. E. Cash, B. Monks, and J. E. Russell.** 1996. Developmental silencing of the embryonic ζ-globin gene: concerted action of the promoter and the 3′-flanking region combined with stage-specific silencing by the transcribed segment. Mol. Cell. Biol. **16:**2637–2646.
34. **Meyuhas, O., and R. P. Perry.** 1980. Construction and identification of cDNA clones for mouse ribosomal proteins: application for the study of r-protein gene expression. Gene **10:**113–129.
35. **Mueller, B. U., T. Pabst, J. Fos, V. Petkovic, M. F. Fey, N. Asou, U. Buergi, and D. G. Tenen.** 2006. ATRA resolves the differentiation block in t(15;17) acute myeloid leukemia by restoring PU.1 expression. Blood **107:**3330–3338.
36. **Muglia, L., and J. Locker.** 1984. Developmental regulation of albumin and alpha-fetoprotein gene expression in rat. Nucleic Acids Res. **12:**6751–6762.
37. **Nielsen, L. B., D. Kahn, T. Duell, H. U. Weier, S. Taylor, and S. G. Young.** 1998. Apolipoprotein B gene expression in a series of human apolipoprotein B transgenic mice generated with recA-assisted restriction endonuclease

cleavage-modified bacterial artificial chromosomes. An intestine-specific enhancer element is located between 54 and 62 kilobases 5′ to the structural gene. J. Biol. Chem. **273:**21800–21807.
38. **Niwa, Y., M. Matsumura, Y. Shiratori, M. Imamura, N. Kato, S. Shiina, T. Okudaira, Y. Ikeda, T. Inoue, and M. Omata.** 1996. Quantitation of alpha-fetoprotein and albumin messenger RNA in human hepatocellular carcinoma. Hepatology **23:**1384–1392.
39. **Parrizas, M., M. A. Maestro, S. F. Boj, A. Paniagua, R. Casamitjana, R. Gomis, F. Rivera, and J. Ferrer.** 2001. Hepatic nuclear factor 1-alpha directs nucleosomal hyperacetylation to its tissue-specific transcriptional targets. Mol. Cell. Biol. **21:**3234–3243.
40. **Pramfalk, C., M. A. Davis, M. Eriksson, L. L. Rudel, and P. Parini.** 2005. Control of ACAT2 liver expression by HNF1. J. Lipid Res. **46:**1868–1876.
41. **Raynal, F., B. Michot, and J. P. Bachellerie.** 1984. Complete nucleotide sequence of mouse 18 rRNA gene: comparison with other available homologs. FEBS Lett. **167:**263–268.
42. **Silverman, E., S. Eimerl, and J. Orly.** 1999. CCAAT enhancer-binding protein beta and GATA-4 binding regions within the promoter of the steroidogenic acute regulatory protein (StAR) gene are required for transcription in rat ovarian cells. J. Biol. Chem. **274:**17987–17996.
43. **Song, Y.-H., A. K. Naumova, S. A. Liebhaber, and N. E. Cooke.** 1999. Physical and meiotic mapping of the region of human chromosome 4q11-q13 encompassing the vitamin D binding protein DBP/Gc-globulin and albumin multigene cluster. Genome Res. **9:**581–587.
44. **Song, Y. H., K. Ray, S. A. Liebhaber, and N. E. Cooke.** 1998. Vitamin D-binding protein gene transcription is regulated by the relative abundance of hepatocyte nuclear factors 1α and 1β. J. Biol. Chem. **273:**28408–28418.
45. **Soutoglou, E., G. Papafotiou, N. Katrakili, and I. Talianidis.** 2000. Transcriptional activation by hepatocyte nuclear factor-1 requires synergism between multiple coactivator proteins. J. Biol. Chem. **275:**12515–12520.
46. **Soutoglou, E., and I. Talianidis.** 2002. Coordination of PIC assembly and chromatin remodeling during differentiation-induced gene activation. Science **295:**1901–1904.
47. **Soutoglou, E., B. Viollet, M. Vaxillaire, M. Yaniv, M. Pontoglio, and I. Talianidis.** 2001. Transcription factor-dependent regulation of CBP and P/CAF histone acetyltransferase activity. EMBO J. **20:**1984–1992.
48. **Strahl, B. D., and C. D. Allis.** 2000. The language of covalent histone modifications. Nature **403:**41–45.
49. **Tanaka, T., Y. Tomaru, Y. Nomura, H. Miura, M. Suzuki, and Y. Hayashizaki.** 2004. Comprehensive search for HNF-1beta-regulated genes in mouse hepatoma cells perturbed by transcription regulatory factor-targeted RNAi. Nucleic Acids Res. **32:**2740–2750.
50. **Wang, N. D., M. J. Finegold, A. Bradley, C. N. Ou, S. V. Abdelsayed, M. D. Wilde, L. R. Taylor, D. R. Wilson, and G. J. Darlington.** 1995. Impaired energy homeostasis in C/EBP alpha knockout mice. Science **269:**1108–1112.
51. **White, P., and N. E. Cooke.** 2000. The multifunctional properties and characteristics of vitamin D-binding protein. Trends Endocrinol. Metab. **11:**320–327.
52. **Yoshida, Y., D. E. Hughes, F. M. Rausa III, I. M. Kim, Y. Tan, G. J. Darlington, and R. H. Costa.** 2006. C/EBPalpha and HNF6 protein complex formation stimulates HNF6-dependent transcription by CBP coactivator recruitment in HepG2 cells. Hepatology **43:**276–286.
53. **Zhou, L., A. A. Nazarian, and S. T. Smale.** 2004. Interleukin-10 inhibits interleukin-12 p40 gene transcription by targeting a late event in the activation pathway. Mol. Cell. Biol. **24:**2385–2396.